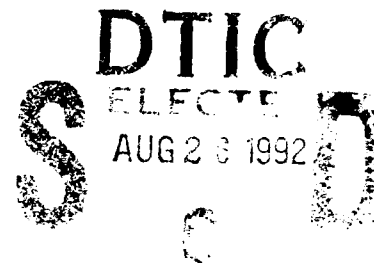




# A PROPOSED GAS RELEASE EXPERIMENT ON THE ARGOS SATELLITE

Shu T. Lai  
Edmond Murad  
C. P. Pike



29 January 1992

---

APPROVED FOR PUBLIC RELEASE; DISTRIBUTION UNLIMITED.

---

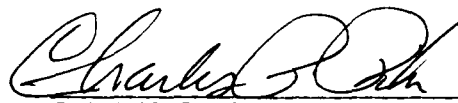
92-23674



**PHILLIPS LABORATORY**  
**DIRECTORATE OF GEOPHYSICS**  
AIR FORCE SYSTEMS COMMAND  
HANSCOM AIR FORCE BASE, MA 01731-5000

This technical report has been reviewed and is approved for publication.

  
Branch Chief

  
CHARLES P. PIKE  
Chief, Spacecraft Interactions Branch (WSSI)

This report has been reviewed by the ESD Public Affairs Office (PA) and is releasable to the National Technical Information Service (NTIS).

Qualified requestors may obtain additional copies from the Defense Technical Information Center. All others should apply to the National Technical Information Service.

If your address has changed, or if you wish to be removed from the mailing list, or if the addressee is no longer employed by your organization, please notify PL/TSI, Hanscom AFB, MA 01731. This will assist us in maintaining a current mailing list.

Do not return copies of this report unless contractual obligations or notices on a specific document requires that it be returned.

**REPORT DOCUMENTATION PAGE**Form Approved  
OMB No. 0704-0188

Public reporting for this collection of information is estimated to average 1 hour per response, including the time for reviewing instructions, searching existing data sources, gathering and maintaining the data needed, and completing and reviewing the collection of information. Send comments regarding this burden estimate or any other aspect of this collection of information, including suggestions for reducing this burden, to Washington Headquarters Services, Directorate for Information Operations and Reports, 1215 Jefferson Davis Highway, Suite 1204, Arlington, VA 22202-4302, and to the Office of Management and Budget, Paperwork Reduction Project (0704-0188), Washington, DC 20503.

1. AGENCY USE ONLY (Leave blank)		2. REPORT DATE 29 January 1992	3. REPORT TYPE AND DATES COVERED Scientific Interim	
4. TITLE AND SUBTITLE  A Proposed Gas Release Experiment on the ARGOS Satellite			5. FUNDING NUMBERS  PE 62101F 76013006	
6. AUTHOR(S)  Shu T. Lai, Edmond Murad, C.P. Pike				
7. PERFORMING ORGANIZATION NAME(S) AND ADDRESS(ES)  Phillips Laboratory (WSSI) Hanscom AFB, MA 01731-5000			8. PERFORMING ORGANIZATION REPORT NUMBER  PL-TR-92-2058 ERP, No. 1098	
9. SPONSORING/MONITORING AGENCY NAME(S) AND ADDRESS(ES)			10. SPONSORING/MONITORING AGENCY REPORT NUMBER	
11. SUPPLEMENTARY NOTES				
12a. DISTRIBUTION/AVAILABILITY STATEMENT  Approved for public release; distribution unlimited.			12b. DISTRIBUTION CODE	
13. ABSTRACT (Maximum 200 words)  We propose to release xenon and carbon dioxide gases from nozzles on the Advanced Research and Global Observaton Satellite (ARGOS) satellite orbiting with a velocity of about 7.4 km/s at an altitude of about 800 km. The releases will be conducted mostly in darkness over the Maui telescope site. The vector sum of the satellite and gas velocities will exceed the velocity requirement for the critical ionization velocity (CIV) process of xenon. It is feasible that the xenon gas will achieve critical velocity ionization. Associative ionization and collisional stripping will not occur for the xenon gas and there is no photo-ionization in darkness; ionization processes competing with CIV are absent. Neutral density, ambient magnetic field, and seed ionization effects on the xenon gas CIV will be discussed. Unlike xenon, carbon dioxide will not undergo CIV because of its higher velocity requirement. However, it is feasible that carbon dioxide colliding with the atmospheric species will form excited CO and OH molecules, which will radiate subsequently. Optical, IR, and UV observatons on the satellite and at Maui will provide diagnostic measurements for the experiment.				
14. SUBJECT TERMS Critical ionization velocity, Gas release, Satellite, Advanced Research and Global Observation Satellite (ARGOS)			15. NUMBER OF PAGES 42	
			16. PRICE CODE	
17. SECURITY CLASSIFICATION OF REPORT UNCLASSIFIED	18. SECURITY CLASSIFICATION OF THIS PAGE UNCLASSIFIED	19. SECURITY CLASSIFICATION OF ABSTRACT UNCLASSIFIED	20. LIMITATION OF ABSTRACT SAR	

# DISCLAIMER NOTICE



THIS DOCUMENT IS BEST QUALITY AVAILABLE. THE COPY FURNISHED TO DTIC CONTAINED A SIGNIFICANT NUMBER OF COLOR PAGES WHICH DO NOT REPRODUCE LEGIBLY ON BLACK AND WHITE MICROFICHE.

## Preface

The authors are grateful to W.J. McNeil and A. Setayesh for particle-in-cell plasma simulations of xenon CIV and Monte Carlo simulations of CO<sub>2</sub> respectively. We would like to thank J. Elgin for providing a Monte Carlo computer simulation code with which we accomplish our carbon dioxide gas release simulation task.

We presented part of this report at the AGU Fall Meeting, San Francisco, CA, 9 December 1991.

Accession For	
DTIC TAB	<input checked="" type="checkbox"/>
Unannounced	<input type="checkbox"/>
By Mail	<input type="checkbox"/>
Availability Codes	
Avail and/or	
Dist	Special
A-1	

## Contents

1. INTRODUCTION	1
2. THE ARGOS SATELLITE	2
3. XENON GAS RELEASE	2
3.1 Critical Ionization Velocity	2
3.2 Plasma Instability	5
3.3 Seed Ionization	7
3.4 Release Rate	8
3.5 Release Directions	10
3.6 Townsend's Criterion	11
3.7 Altitude Effects	15
3.8 Spectral Lines	17
3.9 Mass Loading	18
3.10 Plasma Simulation	19
3.11 Physical Interpretation	22
4. CARBON DIOXIDE RELEASE	25
4.1 Reaction with Atomic O and H	25
4.2 Reaction Energetics	25
4.3 Monte Carlo Simulation	26
5. CONCLUSION	27
REFERENCES	

## Illustrations

1. The Proposed ARGOS Satellite CIV Experiment Over Maui	3
2. Directions of Gas Releases From ARGOS in the Proposed Experiment	4
3. A Schematic Diagram of CIV	4
4. A Schematic Diagram of the Plasma Process in CIV. The electrons are accelerated by plasma waves	6
5. (Upper) Vector Diagram of the Satellite and Gas Velocities (Lower) Geometry of the Gas Velocity Pitch angle $\phi$	10
6. Perpendicular Component $V_{\perp}$ of Gas Velocity in Space and the Pitch Angle $\phi$	12
7. Numerical Results for $x_c$ for various hypothetical, conical, gas release rates in grams per 300 ms [from <i>Lai and Murad</i> , 1989]	13
8. An Example of Energy Loss to Line Excitation (for Ba Gas) as a Function of Altitude [from <i>Lai et al</i> , 1992]	16
9. An Example of Charge Exchange Rate $r(h)$ (for NO Gas) at Altitude $h$ Normalized to $r(h_0)$ at $h_0 = 300$ km [from <i>Lai et al</i> , 1992]	17
10. Momentum Coupling Between Beam Ions and the Ambient Ions in a Flux Tube	19
11. Simulation Results of Charge Build up in a Neutral Cloud as a Result of Charge Exchange with the Ambient Atomic $O^+$	21
12. Simulation Results of Xenon CIV. Metastable states, line excitation, charge exchange, and of course, electron impact ionization have been taken into account	23

13. The Center of Mass Energy Range, Bracketed by the Forward and Backward Release Cases, for the Collision $\text{CO}_2 + \text{O}$	27
14. The Center of Mass Energy Range, Bracketed by the Forward and Backward Release Cases, for the Collision $\text{CO}_2 + \text{H}$	28
15. Experimental ( - ) and Calculated ( --- ) Emission Spectra in the $^1\text{B}_2 \rightarrow ^1\text{A}_1$ Transition of $\text{CO}_2$ for the Collision $\text{CO}_2 + \text{O}$ [from Orient et al, 1990]	29
16. Results of Monte Carlo Simulation of $\text{CO}_2 + \text{O} \rightarrow \text{CO}^* + \text{O}_2$ Showing the CO Vibrational Emission at $4.6 \mu\text{m}$	30
17. Results of Monte Carlo Simulation of $\text{CO}_2 + \text{H} \rightarrow \text{OH}^* + \text{CO}$ Showing the OH Vibrational Emission at $2.7 \mu\text{m}$	31

## Tables

1. Important Natural Parameters for the CIV Experiment on ARGOS	7
2. Important Design Parameters for the CIV Experiment on ARGOS	9
3. Simulation Parameters	22



# A Proposed Gas Release Experiment on the ARGOS Satellite

## 1. INTRODUCTION

Artificial modification and ionization enhancement in the ionosphere may result in local ionospheric irregularities that may control or interfere with radio wave propagation, generate tell-tale infrared signatures, enhance or degrade existing ionospheric irregularities, and produce a wide variety of phenomena through non-linear processes.<sup>1</sup> In our proposed experiment, we plan to release xenon and carbon dioxide gases into the atmosphere from the Advanced Research and Global Observation Satellite (ARGOS) to study (1) the critical ionization velocity (CIV) process<sup>2</sup> of xenon gas and (2) the chemical reactions of CO<sub>2</sub> gas. In this report, we discuss the main points of the proposed experiment and present a feasibility study.

---

Received for publication 24 January 1992

<sup>1</sup> Bernhardt, P., Tepley, C.A., and Duncan, L.M. (1989) Airglow enhancements associated with plasma cavities formed during ionospheric heating experiments, *J. Geophys. Res.*, **94**:9071.

<sup>2</sup> Alfvén, H. (1960) Collision between a non-ionized gas and a magnetized plasma, *Rev. Mod. Phys.*, **32**:710-713.

## 2. THE ARGOS SATELLITE

The satellite will be in a circular orbit at an altitude of about 450 nmi. (835 km) with an orbital velocity of 7.4 km/s. The gas release experiment will be one of several experiments to be conducted onboard the satellite. It will be conducted when the satellite is passing over Maui, Hawaii, where the AMOS telescope will observe the experiment (Figure 1).

## 3. XENON GAS RELEASE

Xenon gas will be released in four different directions (Figure 2). The purpose of the experiment is to study the signatures of enhanced ionization due to the CIV process.

### 3.1 Critical Ionization Velocity

Alfvén<sup>3</sup> proposed the hypothesis of critical ionization velocity (CIV) – when a neutral gas travels through a magnetized plasma with a relative velocity exceeding a critical value, rapid ionization of the neutral gas occurs. The critical value of the velocity is called the critical ionization velocity  $V_*$ , and is given by:<sup>3</sup>

$$V_* = \sqrt{(2e\Phi/M)} \quad (1)$$

where  $e\Phi$  is the ionization energy and  $M$  is the mass of a neutral particle (Figure 3).  $V_*$  is the minimum value of  $V_\perp$  to cause ionization, where  $V_\perp$  is the relative velocity component perpendicular to the magnetic field. For xenon,  $e\phi = 12.13$  eV,  $M = 131.3$  AMU, and  $V_* = 4.225$  km/s.

---

<sup>3</sup> Alfvén, H. (1954) *On the Origin of the Solar System*, Oxford Univ. Press, Oxford.

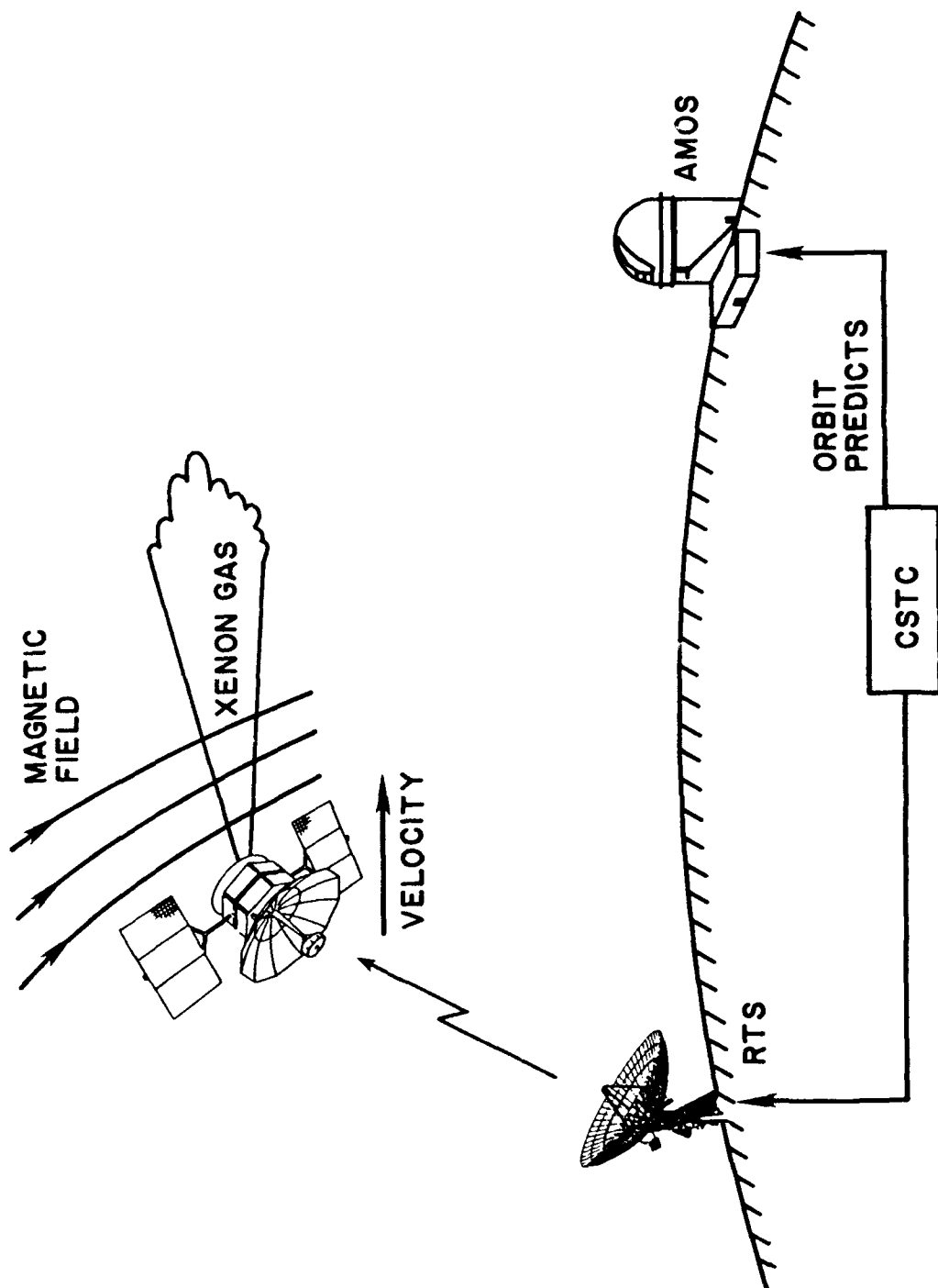


Figure 1. The Proposed ARGOS Satellite CIV Experiment Over Maui

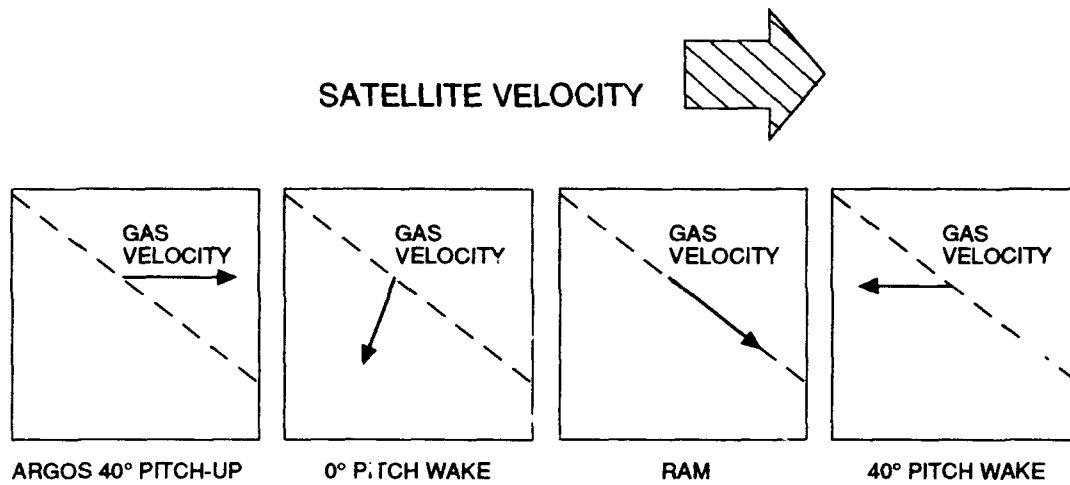


Figure 2. Directions of Gas Releases From ARGOS in the Proposed Experiment

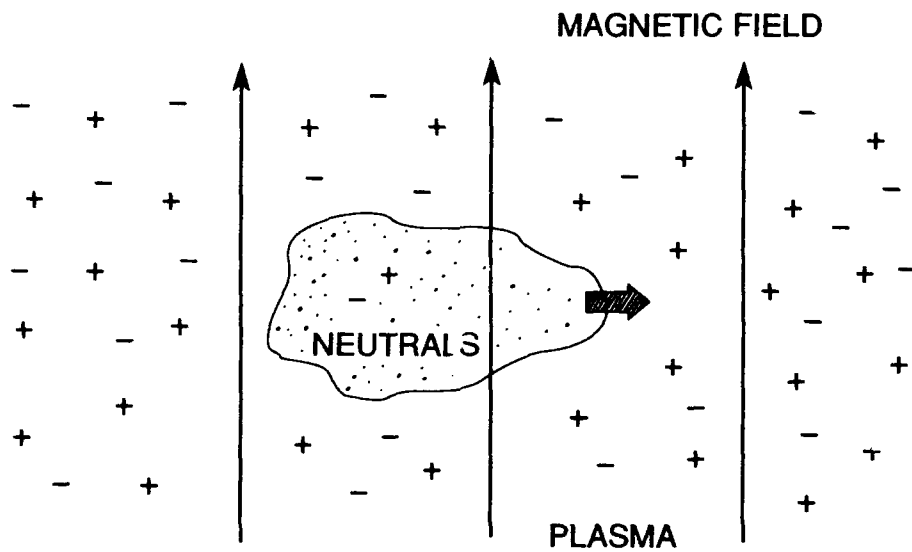


Figure 3. A Schematic Diagram of CIV

Möbius et al<sup>4</sup> first suggested that since spacecraft velocity may be close to  $V_c$ , the vector sum of the spacecraft and gas velocities may equal or exceed  $V_c$ . Axnäs<sup>5</sup> worked out some necessary conditions for a CIV interaction between the ionospheric plasma and a xenon cloud. Murad et al<sup>6</sup> suggested releasing four gases from the Space Shuttle for testing CIV in space.

### 3.2 Plasma Instability

The CIV process is generally accepted to be mediated by some beam-plasma instability, such as the two-stream plasma instability<sup>7,8,9</sup> that occurs when a neutral beam (with ions and electrons in it) travels across an ambient magnetic field (Figure 4). The beam-plasma instability waves, energized by the ion beam, accelerate electrons. According to quasi-linear plasma theory, the electrons form a plateau-tail distribution.<sup>10</sup> Some of the 'hot' electrons in the tail may be energetic enough to ionize the neutrals by impact. As ionization occurs, new ions are created. When they are created, they have the velocity of the neutrals. They carry on the CIV process by energizing the beam-plasma instability waves, which in turn energize the electrons. Thus, CIV is a cyclic process, in which a neutral gas is ionized by means of its own kinetic energy.

---

<sup>4</sup> Möbius, E., Boswell, R.W., Piel, A., and Henry, P. (1979) A spacelab experiment on the critical ionization velocity, *Geophys. Res. Lett.*, **6**:29.

<sup>5</sup> Axnäs, I. (1980) Some necessary conditions for a critical velocity interaction between the ionospheric plasma and a xenon cloud, *Geophys. Res. Lett.*, **7**:933-936.

<sup>6</sup> Murad, E., Lai, S.T., and Stair, A.T. (1986) An experiment to study the critical ionization velocity theory in space, *J. Geophys. Res.*, **91**:A9 10188-10192.

<sup>7</sup> Möbius, E., Papadopoulos, K., and Piel, A. (1987) On the turbulent heating and the threshold condition in the critical ionization velocity interaction, *Planet. Space Science*, **35**:345.

<sup>8</sup> Goertz, C.K., Machida, S., and Lu, G. (1990) On the theory of CIV, *Adv. Space Res.*, 33-46.

<sup>9</sup> McNeil, W.J., Lai, S.T., and Murad, E. (1990) Interplay between collective and collisional processes in critical velocity ionization, *J. Geophys. Res.*, **95**:A7 103435-10354.

<sup>10</sup> Formisano, V., Galeev, A.A., and Sagdeev, R.Z. (1982) The role of the critical ionization velocity phenomenon in the production of the inner coma cometary plasma, *Planet. Space Sci.*, **30**:491-497.

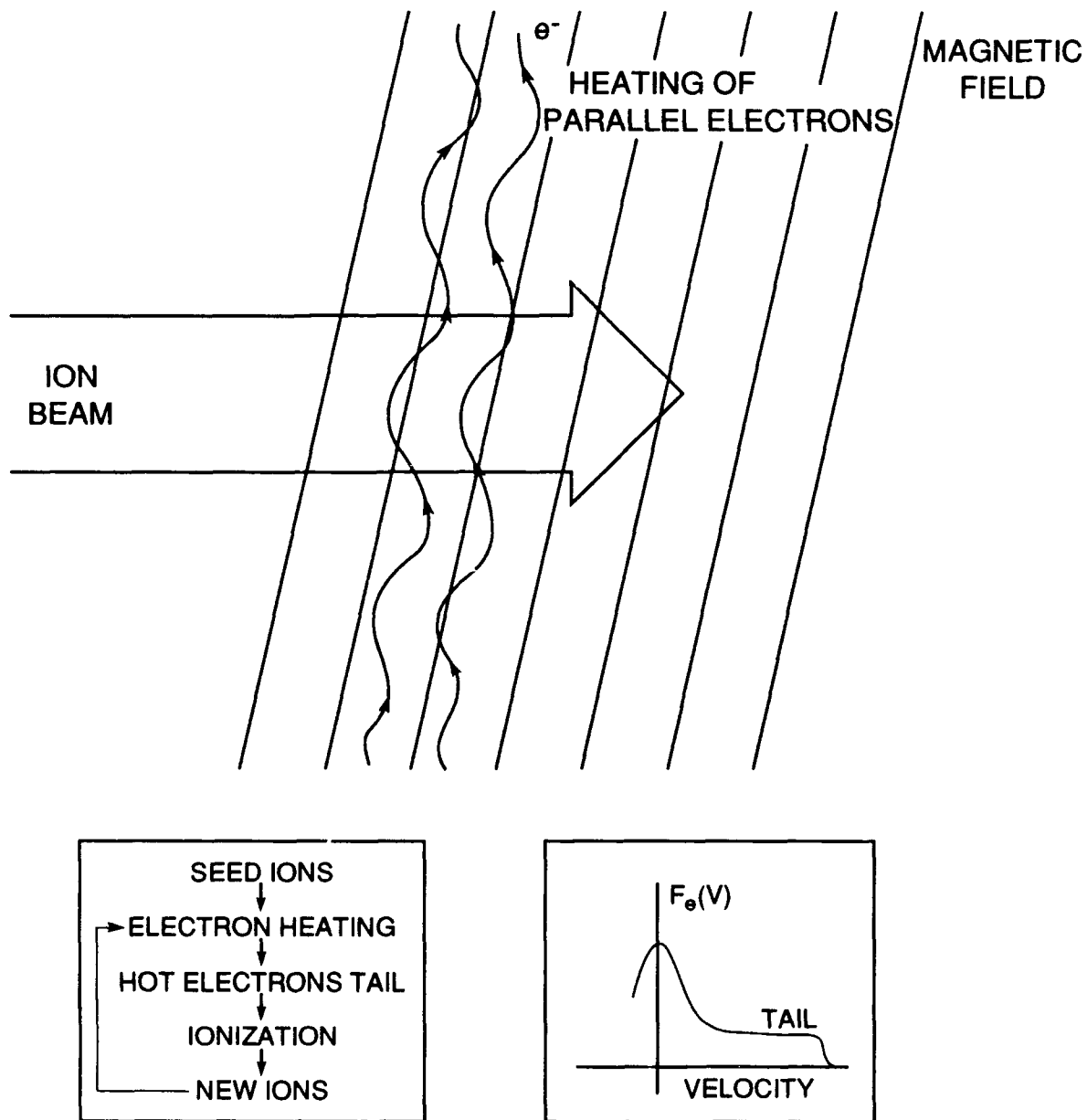


Figure 4. A Schematic Diagram of the Plasma Process in CIV. The electrons are accelerated by plasma waves.

In the proposed experiment on ARGOS, the gyrofrequency of xenon is expected to be about 4.2 Hz, the gyroradius 282 m, and the lower hybrid plasma frequency about 2.05 kHz. Some important parameters for the ARGOS CIV experiment are listed in Table 1.

Table 1. Important Natural Parameters for the CIV Experiment on ARGOS

Xenon Mass	131.3 AMU
Xenon Ionization Potential	12.13 eV
Xenon Critical Ionization Velocity $V_*$	4.225 km/s
Altitude	835 km
Nighttime Ambient $H^+$ Density	$2 \times 10^4$ /cc.
Daytime Ambient $O^+$ density	$2 \times 10^4$ /cc.
Nighttime Ambient Electron Density	$2 \times 10^4$ /cc.
Daytime Ambient Electron Density	$5 \times 10^5$ /cc.
Magnetic Field Magnitude at Maui	0.36 G
Magnetic Field Declination	$11^\circ$
Magnetic Field Inclination	$38.7^\circ$
Electron Gyrofrequency	$1006 \times 10^6$ Hz
Xenon Gyrofrequency	4.17 Hz
Xenon Gyroradius	282.4 m
Xenon Lower Hybrid Frequency	2.047 kHz

### 3.3 Seed Ionization

To begin with, the neutral gas must have seed ionization, otherwise no plasma interaction will occur. In the proposed experiment, there is no thermal ionization by explosions, stripping ionization is energetically impossible at the gas velocity used, and photoionization is ruled out because the ionization potential (12.13 eV) of xenon is higher than the Lyman- $\alpha$  line energy (10.2 eV) of sunlight. Seed ions can come only from charge exchange with the ambient plasma. In the daytime, the charge exchange<sup>11</sup> is between Xe and ambient  $O^+$ , the cross section being  $\sigma_{O^+} = 4.8 \times 10^{-16}$  cm<sup>2</sup>. The density of  $O^+$  at 835 km altitude is typically  $2 \times 10^4$  /cc. At night, the charge exchange is between Xe and ambient  $H^+$ , the cross section<sup>12</sup> being  $\sigma_{H^+} \approx 1.5 \times 10^{-16}$  cm<sup>2</sup> and density of  $H^+ \approx 2 \times 10^4$  /cc. Assuming that the ions leave the beam in  $1/4$  gyroperiod  $\tau_B$ , the number density  $n_i$  of xenon ions generated by charge exchange is given by

$$n_i(t) = \int_0^{\tau_B/4} dt n_{Xe} \sigma V n_{\text{ambient}} \quad (2)$$

<sup>11</sup> Jönsson, B.O. (1980) private communication to I. Axnäs.

<sup>12</sup> de Heer, F.J., Jansen, R.H.J., and van der Kaay, W. (1979) *J. Phys. B*, 12:979-1002.

where  $n_{Xe}$  and  $n_{ambient}$  are number densities of neutral xenon atoms and ambient ions, respectively, and  $V$  is the relative velocity between Xe and the ambient ions. Suppose the ambient ions have a zero velocity and the xenon atoms travel at a velocity  $V$  equal to the maximum vector sum of the satellite velocity (7.4 km/s) plus the gas exit velocity (0.4 km/s). We obtain  $V \approx 7.8$  km/s. The neutral gas density is assumed to be  $10^9$ /cc. The result of Eq. (2) is

$$n_i \approx 3.7 \times 10^2 / \text{cc (Day)}$$

and

$$n_i \approx 1.2 \times 10^2 / \text{cc (Night)} .$$

Therefore the ratios  $p$  of seed ions to ambient ions are approximately:

$$p(\text{Day}) = 3.7\%$$

$$p(\text{Night}) = 1.2\% .$$

The estimated results,  $p(\text{Day})$  and  $p(\text{Night})$ , would be higher if one takes into account ambipolar diffusion and other mechanisms of electron or ion confinement, because these mechanisms may slow down the escape of electrons or ions. More accurate measurement of cross sections would also help to improve the estimated result.

### 3.4 Release Rate

In thermodynamics, the velocity  $V$  of molecules of mass  $M$  at temperature  $T$  °K is given by<sup>13</sup>

$$V(T) = \int_0^\infty dV V f_T(V) = \left( \frac{8kT}{\pi M} \right)^{1/2} . \quad (3)$$

---

<sup>13</sup> Reidl, P.C. (1988) *Thermal Physics*, 2nd edition, Oxford University Press, Oxford.



We have assumed a Maxwellian distribution  $f_T(V)$  to obtain the result in Eq. (3). For a 0°C xenon gas,  $kT = 1.38 \times 10^{-16} \times 273 \text{ gm cm}^2/\text{s}^2$ . The xenon mass  $M$  is  $131.3 \times 1.67 \times 10^{-24} \text{ gm}$ . Using these numbers as input, Eq. (3) gives the xenon gas velocity  $V(\text{Xe}) = 210 \text{ m/s}$  at the exit point. Similarly, for the  $\text{CO}_2$  gas, its molecular weight being 44, the gas velocity  $V(\text{CO}_2) = 362 \text{ m/s}$ .

In thermodynamics, the pressure  $p(M,T)$  is given by

$$p = \frac{1}{3} \rho V^2 \quad (4)$$

where  $\rho$  ( $= nm$ ) is the mass density, and  $n$  is the number density of the gas. For a 10 atmosphere xenon gas,  $p = 10^7 \text{ gm cm}^{-1}\text{s}^{-2}$ . The mass density  $\rho$  (which is given by  $\rho = 3p/V^2$ ) of the xenon gas is  $\rho(\text{Xe}) = 0.068 \text{ gm/cc}$ . Similarly, for the  $\text{CO}_2$  gas,  $\rho(\text{CO}_2) = 0.023 \text{ gm/cc}$ .

The mass release rate  $R$ , which is given by  $R = AV\rho$ , depends on the cross section  $A$  of the nozzle. For a nozzle of  $1/4 \text{ cm}$  radius,  $A = \pi(1/4)^2 \text{ cm}^2$ . Using the above values of  $V$ ,  $\rho$ , and  $A$  as input, we obtain  $R(\text{Xe}) = 280 \text{ gm/s}$  or  $84 \text{ gm/(300ms)}$ ;  $R(\text{CO}_2) = 162 \text{ gm/s}$  or  $48.6 \text{ gm/(300ms)}$ . The particle number release rates  $N_R$  are calculated to be  $N_R(\text{Xe}) = 1.27 \times 10^{24}/\text{s}$  and  $N_R(\text{CO}_2) = 3.8 \times 10^{24}/\text{s}$ .

Some important design parameters in the ARGOS CIV experiment are listed in Table 2. The values in square brackets correspond to 77° gas temperature.

Table 2. Important Design Parameters for the CIV Experiment on ARGOS

Satellite Velocity	7.4 km/s
Satellite Altitude	Approx 835 km
Satellite Orbit Inclination	98.7°
Gas Pressure at Nozzle	Approx $10^7 \text{ gm cm}^{-1}\text{s}^{-2}$
Nozzle Radius	Approx 0.25 cm (in design)
Gas Temperature	0°C [77°]
Mass Release Rate (Xe)	280 gm/s [249 gm/s]
Mass Release Rate ( $\text{CO}_2$ )	162 gm/s [144 gm/s]
Number Release Rate (Xe)	$1.27 \times 10^{24}/\text{s}$ [ $1.14 \times 10^{24}/\text{s}$ ]
Number Release Rate ( $\text{CO}_2$ )	$2.23 \times 10^{24}/\text{s}$ [ $1.97 \times 10^{24}/\text{s}$ ]
Gas Velocity (Xe)	210 m/s [237 m/s]
Gas Velocity ( $\text{CO}_2$ )	362 m/s [410 m/s]

### 3.5 Release Directions

Since the spacecraft velocity  $V_s$  (7.4 km/s) is much higher than the gas velocity  $V_g$  (0.2 to 0.4 km/s), the vector sum  $V (=V_s + V_g)$  is dominated by  $V_s$  (Figure 5 upper). In the CIV experiment, the kinetic energy available for the excitation of modified two-stream plasma instability is given by the velocity component  $V_{\perp}$  perpendicular to the magnetic field  $B$  (Figure 5 lower). For the CIV process to occur,  $V_{\perp}$  has to exceed the critical ionization velocity  $V_*$  of the gas released. The direction of the earth's magnetic field lines at Maui is given by  $11^\circ$  declination and  $38.7^\circ$  inclination. For given magnitudes of  $V_s$  and  $V_g$ , the component  $V_{\perp}$  depends on the directions of  $V_s$  and  $V_g$  with respect to  $B$ ;  $V_{\perp}$  is maximum when  $V_s$  and  $V_g$  are parallel to each other and exactly perpendicular to  $B$ .

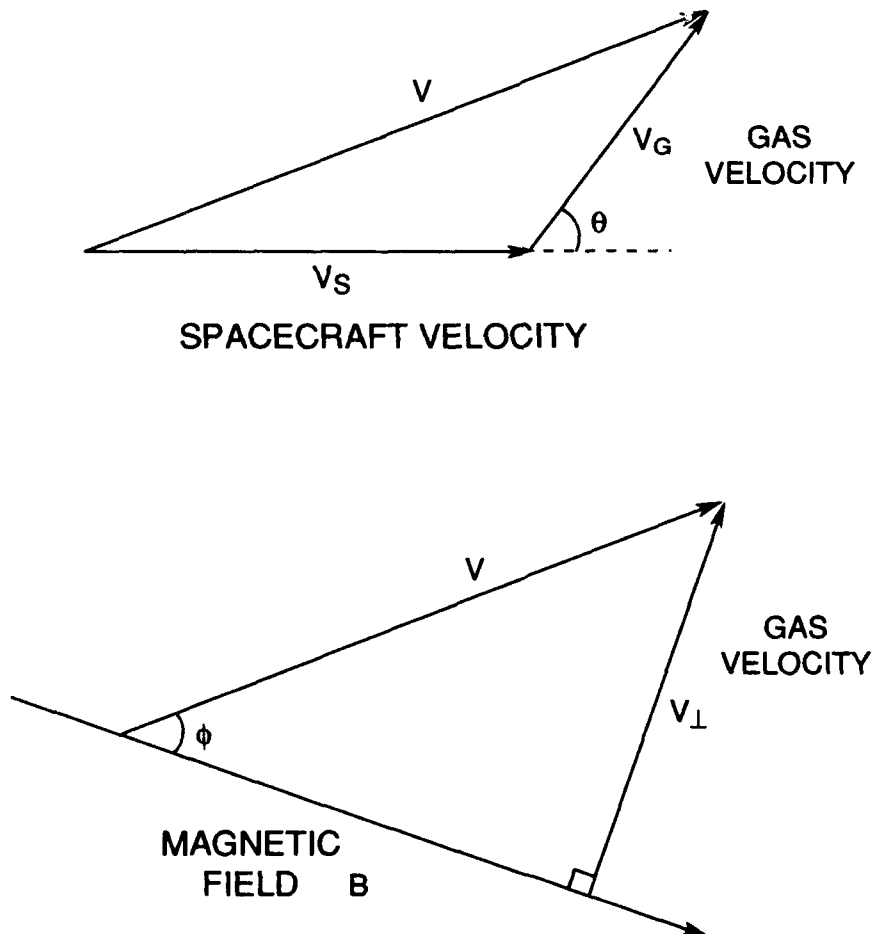


Figure 5. (Upper) Vector Diagram of the Satellite and Gas Velocities. (Lower) Geometry of the Gas Velocity Pitch Angle  $\phi$

For example, suppose the satellite is traveling horizontally. Then,  $V_s$  subtends an angle  $I$  with the magnetic field  $B$ ,  $I$  being the magnetic field inclination. For a given gas release angle  $\theta$  (between  $V_s$  and  $V_g$ ), the velocity component  $V_{\perp}$  and the velocity pitch angle  $\phi$  (between  $V$  and  $B$ ) can be calculated (Figure 6). In this case,  $V_{\perp}$  exceeds  $V_{\perp}(Xe)$ , implying that the kinetic energy requirement for CIV is satisfied, at all values of the release angle  $\theta$ .

### 3.6 Townsend's Criterion

Townsend's criterion<sup>14</sup> states that, to sustain a discharge, an electron has to ionize a neutral at least once during its lifetime  $\tau$  in the interaction region. In the literature of CIV, four Townsend criteria, I to IV, have been suggested.<sup>15</sup> In criterion I,  $\tau$  is governed<sup>16</sup> by the escape of the hot electrons along the magnetic field lines. In criterion II,  $\tau$  is the contact time  $\tau_c$  of a neutral cloud<sup>17</sup> traversing a magnetic field line. The longer the contact time is, the more important is I compared to II. In our proposed CIV experiment, the duration  $\tau_c$  of the neutral gas released is of the order of seconds which is much longer than the electron heating time  $\tau_H$  (order of ms) obtained by using<sup>18</sup> the estimate  $\tau_H \approx 30/\omega_{LH}$ . The other Townsend criteria are less restrictive. We consider criterion I as follows:

Using a conical beam model of half angle  $\phi/2$ , Lai and Murad<sup>16</sup> have formulated the distance within which Townsend's criterion I is satisfied. For the range of release rates in the proposed experiment, the estimated distance within which CIV might occur is of the order of a few meters from the nozzle. Figure 7 shows a typical plot of critical distance for a jet of 3 km/s, cone half angle  $30^\circ$ , and molecular weight 32 amu.

For the xenon gas considered, the velocity is about 7.6 km/s in the space frame, the cone half angle is  $30^\circ$ , and the release rates  $N_R$  have been estimated in Section 4. For simplicity, we let the cross section  $\sigma$  of the electron impact ionization of xenon be  $\sigma(E) = 10^{-16} \text{ cm}^2$  for typical hot electron energies  $E = 10$  to  $30 \text{ eV}$  as expected in a CIV situation. The Townsend critical distance  $X_c = 66 \text{ m}$  from the nozzle point. Beyond  $X_c$ , the neutral gas density is too low to satisfy Townsend's criterion I for CIV.

<sup>14</sup> Townsend, J.S. (1915) *Electricity in Gases*, Clarendon Press, Oxford.

<sup>15</sup> Lai, S.T. and Murad, E. (1992) Inequality conditions for critical velocity ionization space experiments, *IEEE Trans. Plasma Sci.*, in press.

<sup>16</sup> Lai, S.T. and Murad, E. (1989) Critical ionization velocity experiments in space, *Planet. Space Sci.*, **37**:7/865-872.

<sup>17</sup> Brenning, N. (1982) Comment on the Townsend condition, presented at the Workshop on Alfvén's Critical Velocity Effect, Max-Planck Institut für Extraterrestrische Physik, Garching, W. Germany.

<sup>18</sup> Tanaka M. and Papadopoulos, K. (1983) Creation of high energy tails by means of the modified two-stream instability, *Phys. Fluids*, **26**:1697.

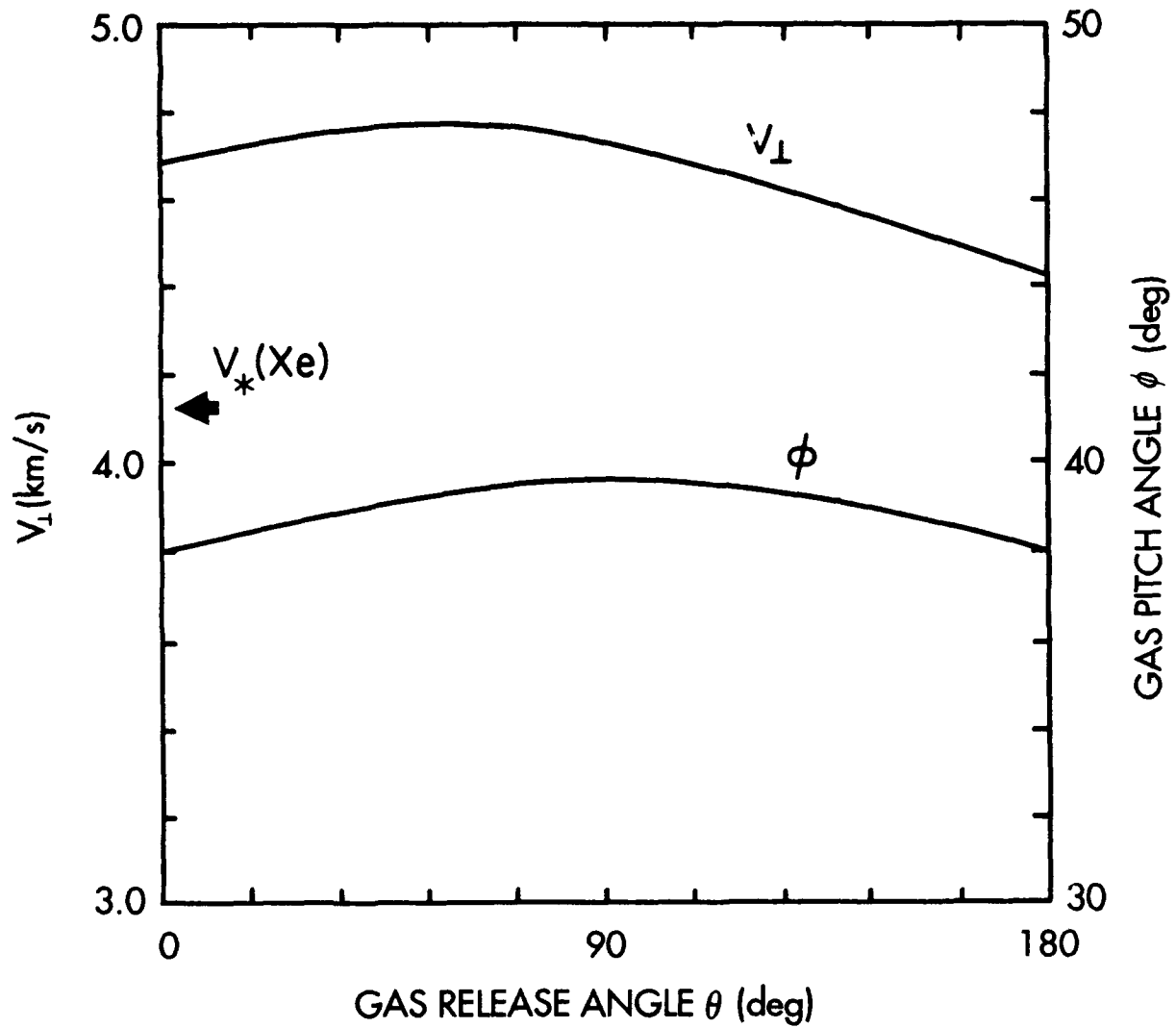


Figure 6. Perpendicular Component  $V_{\perp}$  of Gas Velocity in Space and the Pitch Angle  $\phi$

We now derive a universal formula of Townsend distance  $X_0$  for all masses, assuming that the cross sections of ionization for each species are about the same. From Eqs. (3) and (4), the mass density  $\rho$  is given by

$$\rho = \frac{3\pi pM}{8kT}. \quad (5)$$

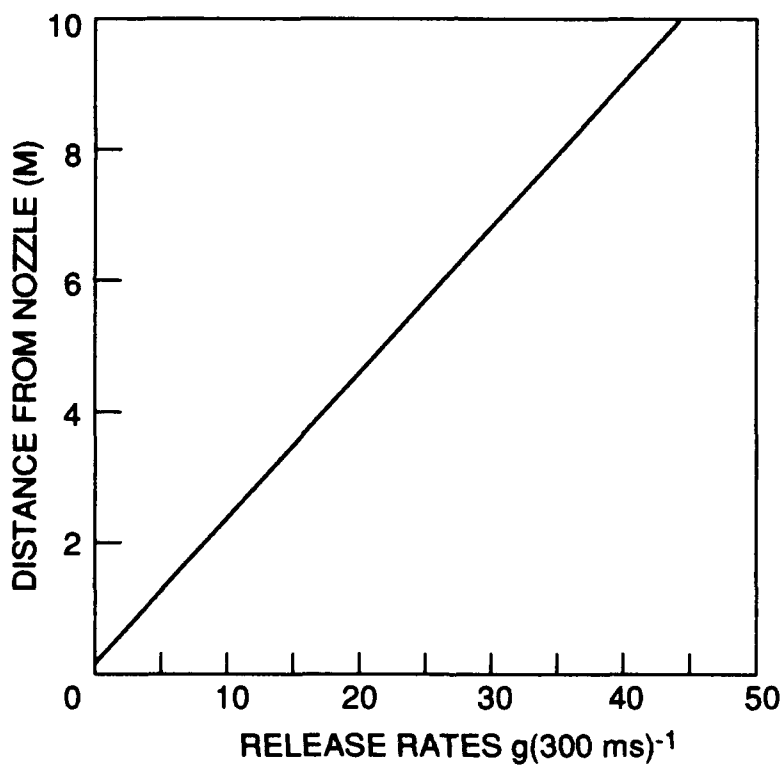
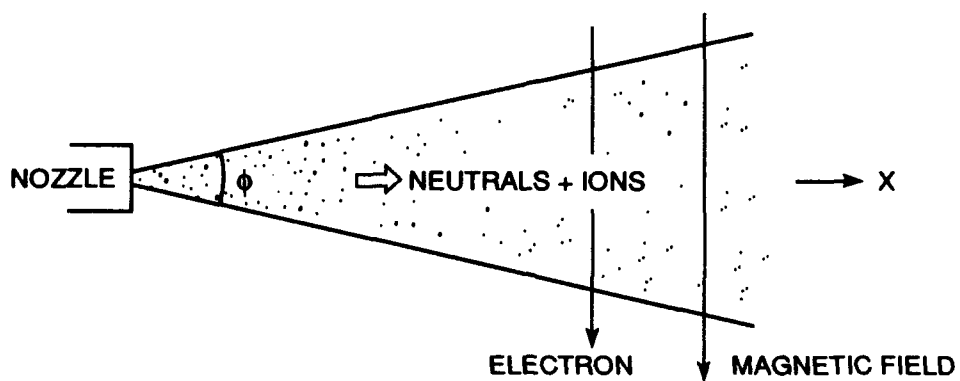


Figure 7. Numerical Results for  $x_c$  for Various Hypothetical, Conical, Gas Release Rates in Grams per 300 ms [from *Lat and Murad*, 1989]

The number release rate  $N_o$  is given by

$$N_o = \frac{R}{M} = \frac{VA\rho}{M} = 1.5Ap \left( \frac{\pi}{2kTM} \right)^{1/2}. \quad (6)$$

In the conical beam model, the number density  $n(x)$  at distance  $x$  from the exit point is given by:<sup>12</sup>

$$n(x) = \frac{N_o}{\pi x^2 V \tan^2(\varphi/2)}. \quad (7)$$

Townsend's criterion requires that the electron impact ionization rate  $v(x)$  and the electron transit time  $\tau(x)$  should satisfy the inequality:

$$v(x)\tau(x) \geq 1 \quad (8)$$

where

$$v(x) = n(x)\sigma(v_e)v_e, \quad (9)$$

and

$$\tau(x) = 2x \tan(\varphi/2) v_e^{-1}, \quad (10)$$

where  $\varphi$  is the full cone angle and  $v_e$  the electron velocity. Using Eqs. (5-9), the universal Townsend critical distance  $x_c$  satisfying Eq. (8) is given by

$$x_c = \frac{2N_o}{\pi V \tan(\varphi/2)} = \frac{1.5\sigma Ap}{2\tan(\varphi/2)kT}. \quad (11)$$

The formula [Eq. (9)] is universal in the sense that it is independent of the molecular mass  $M$ . For example, the critical distance  $x_c$  for a  $\phi = 60^\circ$  beam is

$$x_c = 1.3 \frac{Ap}{kT} \sigma \quad (12)$$

where  $x_c$  is in cm,  $A$  in  $\text{cm}^2$ ,  $p$  in  $\text{gm cm}^{-1}\text{s}^{-2}$  and  $kT$  in  $\text{gm.cm}^2/\text{s}^2$ . For example, we take  $A = \pi(0.25)^2 \text{ cm}^2$ ,  $p = 10 \text{ atm} = 10^7 \text{ gm cm}^{-1}\text{s}^{-2}$ ,  $\sigma \approx 10^{-16} \text{ cm}^2$ ,  $kT = 273 \times 1.38 \times 10^{-16} \text{ gm.cm}^2/\text{s}^2$ . The Townsend critical distance  $x_c$  is 66.7 m from the exit point. This value of  $x_c$  is the same for Xe or  $\text{CO}_2$ , or any gas, as long as the ionization cross section is about the same.

### 3.7 Altitude Effects

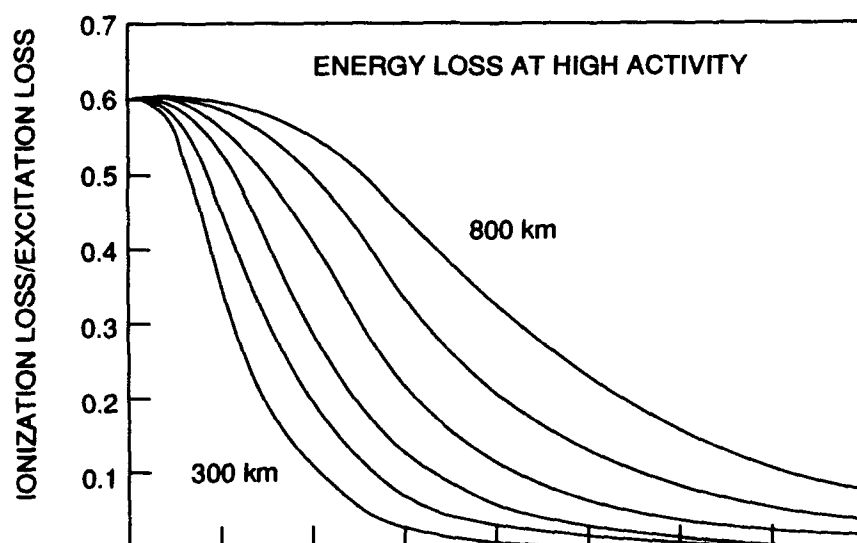
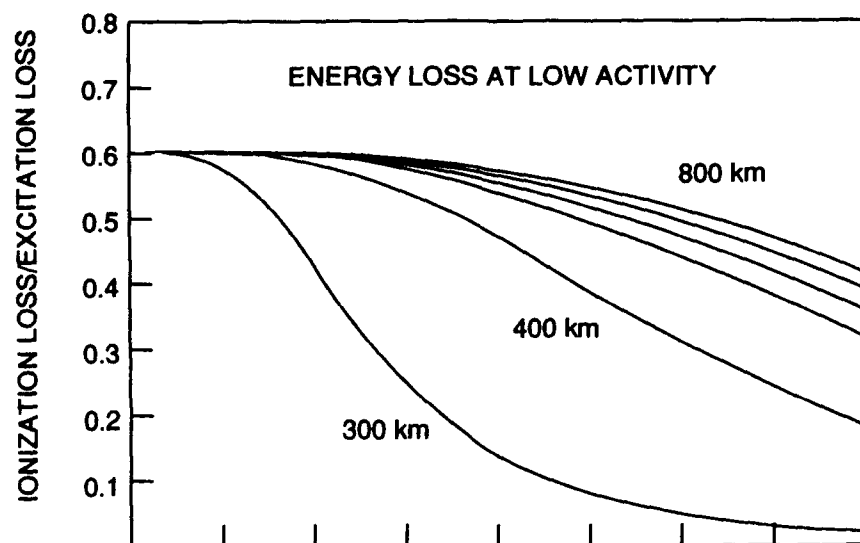
Heretofore, all CIV space experiments were conducted at around 400 to 500 km altitude.<sup>19</sup> There are advantages for conducting CIV experiments at around 800 km instead. The energy loss to line excitation of the ambient neutrals<sup>20</sup> would be less at 800 km. A recent model calculation by Lai et al<sup>21</sup> show that indeed the energy loss to line excitation at 800 km is significantly less than at 500 km (Figure 8). Furthermore, the energy loss to ionization of ambient neutrals is also reduced at 800 km where He ( $\epsilon\phi = 24.6 \text{ eV}$ ) is the dominant species. Since the ambient neutrals, being thermal and not beam-like, do not have a significant net velocity, their ionization would not lead to any significant feedback of directed kinetic energy to the beam-plasma instability and therefore the cyclic process of CIV. Both line excitation and ambient ionization are energy loss mechanisms.

To design an effective CIV space experiment, it is advantageous to avoid the above energy loss mechanisms as much as possible. We suggest, therefore, that conducting CIV experiments at 800 km rather than at the conventional 500 km altitude offers a better likelihood for the CIV experiment to succeed, because the effect of both of the above energy loss mechanisms is less severe at 800 km. There is, however, a disadvantage for CIV experiments at 800 km compared with 500 km; charge exchange, which is important for seed ionization, is less at 800 km (Figure 9).

<sup>19</sup> Tobert, R.B. (1990) Review of critical velocity experiments in the ionosphere, *Adv. Space Res.*, **10**:7/47-58.

<sup>20</sup> Newell, P.T. and Torbert, R.B. (1985) Competing atomic processes in Ba and Sr injection critical velocity experiments, *Geophys. Res. Lett.*, **12**:835.

<sup>21</sup> Lai, S.T., Murad, E., and McNeil, W.J. (1991) Altitude effects in CIV experiments in space, *Planet. Space Sci.*, **39**:12 1707-1713.



TIME(S)	.0	1.0	2.0	3.0	4.0
LOG( $n_{Ba}$ )	26.4	7.2	6.3	5.8	5.4
R(km)	0.0	9.0	18.8	27.8	37.6

Figure 8. An Example of Energy Loss to Line Excitation (for Ba Gas) as a Function of Altitude [from *Lai et al.*, 1992]



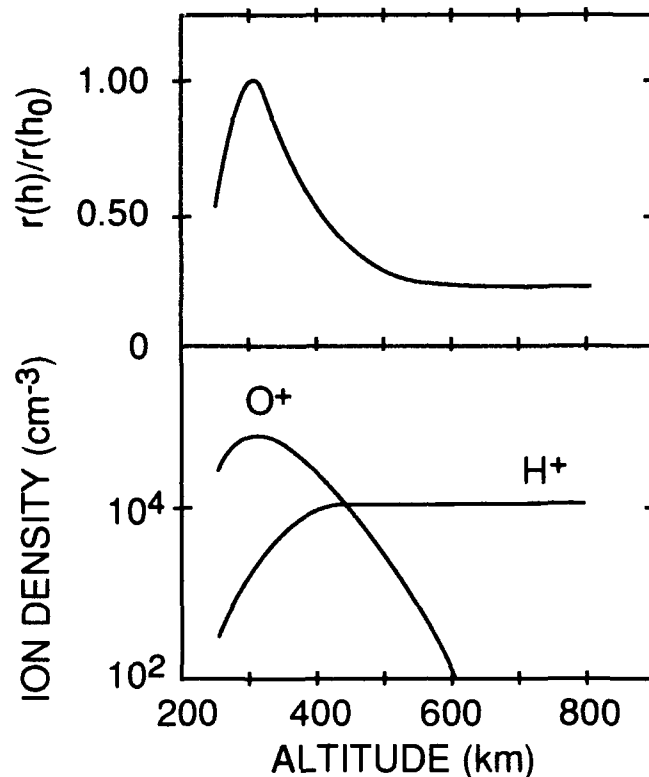


Figure 9. An Example of Charge Exchange Rate  $r(h)$  (for NO Gas) at Altitude  $h$  Normalized to  $r(h_0)$  at  $h_0 = 300$  km [from Lai et al. 1992]

### 3.8 Spectral Lines

Electrons energized to energies above 100 eV have been observed in previous CIV space experiments.<sup>19</sup> If this happens, then we expect  $\text{Xe}^+$ .  $\text{Xe}^+$  has a number of excited states that would be visible from the ground by observing the inter-state emissions. The principal emitters would be the transitions between excited states of  $\text{Xe}^+$ . For example, a scenario for conducting the experiment is to release Xe in sunlight, where the Lyman- $\alpha$  line is not enough to cause ionization. However, once Xe is ionized by electron impact (that is, CIV), the Lyman- $\alpha$  line would pump the  $\text{Xe}^+$  to an upper state from which it would relax to an intermediate state. For example, electron impact of Xe (by CIV) might be expected to give rise to  $\text{Xe}^+(^2\text{P}^o_{1/2})$ . This state is metastable, with a lifetime of 47  $\mu\text{s}$ . It may radiate when it falls to the ground state  $\text{Xe}^+(^2\text{P}^o_{1/2})$  at 987 nm. There are other possibilities. For example, if the CIV discharge forms  $\text{Xe}^+6\text{p}(^2\text{P}^o_{1/2})$ , then we can observe the transition  $\text{Xe}^+6\text{p}(^2\text{P}^o_{1/2}) \rightarrow \text{Xe}^+5\text{p}^5(^2\text{P}^o_{1/2})$  at 30 nm.

### 3.9 Mass Loading

Haerendel<sup>22, 23</sup> pointed out that the newborn ions created by CIV in a neutral beam can drag forward the ambient plasma and the ambient magnetic field lines. The forward drag is a result of the momentum coupling between the beam ions and the ambient ions.

To estimate the critical beam density  $n_{Xe+}$  for momentum coupling to be significant, we equate the ion mass in a beam pulse, modeled as a sphere of radius  $R$ , traveling with a velocity  $V$  and that in an ambient flux tube of length  $D$  (Figure 10). The pulse transit time  $T$  is  $T = R/V$ . Following Haerendel<sup>22</sup> we assume that the length  $D$  is given by the distance traveled by the Alfvén wave in the same duration  $T$ . That is, we assume  $D = TV_A$  where  $V_A$  is the Alfvén velocity. Thus,  $D = R(V_A/V)$ . A simple estimate of the momentum balance can be obtained by considering the tube to be moving at 30 percent of the velocity  $V$  of the beam:

$$M_{Xe+}n_{Xe+}R = M_a n_a R(V_A/V) \times 30 \text{ percent} \quad (13)$$

that is,

$$n_{Xe+} = n_a (M_a/M_{Xe+})(V_A/V) \times 0.3, \quad (14)$$

where  $M$  denotes ion mass,  $n$  ion density, and  $a$ , ambient species. It is interesting to note that Eq. (14) is independent of the beam length  $R$ .

Taking typical parameters at 800 km altitude,<sup>24</sup>  $n_a \approx 10^4/\text{cc}$ ,  $V_A \approx 2000 \text{ km/s}$ ,  $M_H/M_{Xe+} \approx 144$ ,  $V \approx 7.8 \text{ km/s}$ , we obtain  $n_{Xe+} \approx 1 \times 10^7/\text{cc}$ . Thus, for a neutral Xe gas density  $n_{Xe}$  of  $10^9/\text{cc}$  with  $V = 7.8 \text{ km/s}$ , a fractional ionization of  $\alpha = n_{Xe+}/n_{Xe} \approx 1$  percent would invoke mass loading to such an extent that the relative velocity  $V_r$  is reduced to about  $V \times 70$  percent  $\approx 4.5 \text{ km/s}$ . Further increase in ionization  $\alpha$  (beyond  $\alpha \approx 0.01$ ) may reduce the relative velocity  $V_r$  further, rendering the CIV efficiency of about 1 percent nearly zero.

In the above example, mass loading alone already puts a ceiling on the maximum ionization of the xenon beam. Other energy loss mechanisms lower the ceiling even further.

<sup>22</sup> Haerendel, G. (1982) Alfvén's critical velocity effect tested in space, *Z. Naturforsch.*, **37A**:728.

<sup>23</sup> Haerendel, G. (1983) The role of momentum transfer to the ambient plasma in critical velocity experiments, *Active Experiments in Space, Eur. Space Agency Spec. Publ.*, **ESA SP-195**:245.

<sup>24</sup> Kashe, M.A. (1969) *The Ionosphere and Its Interaction with Satellites*, Gordon and Breach, NY.

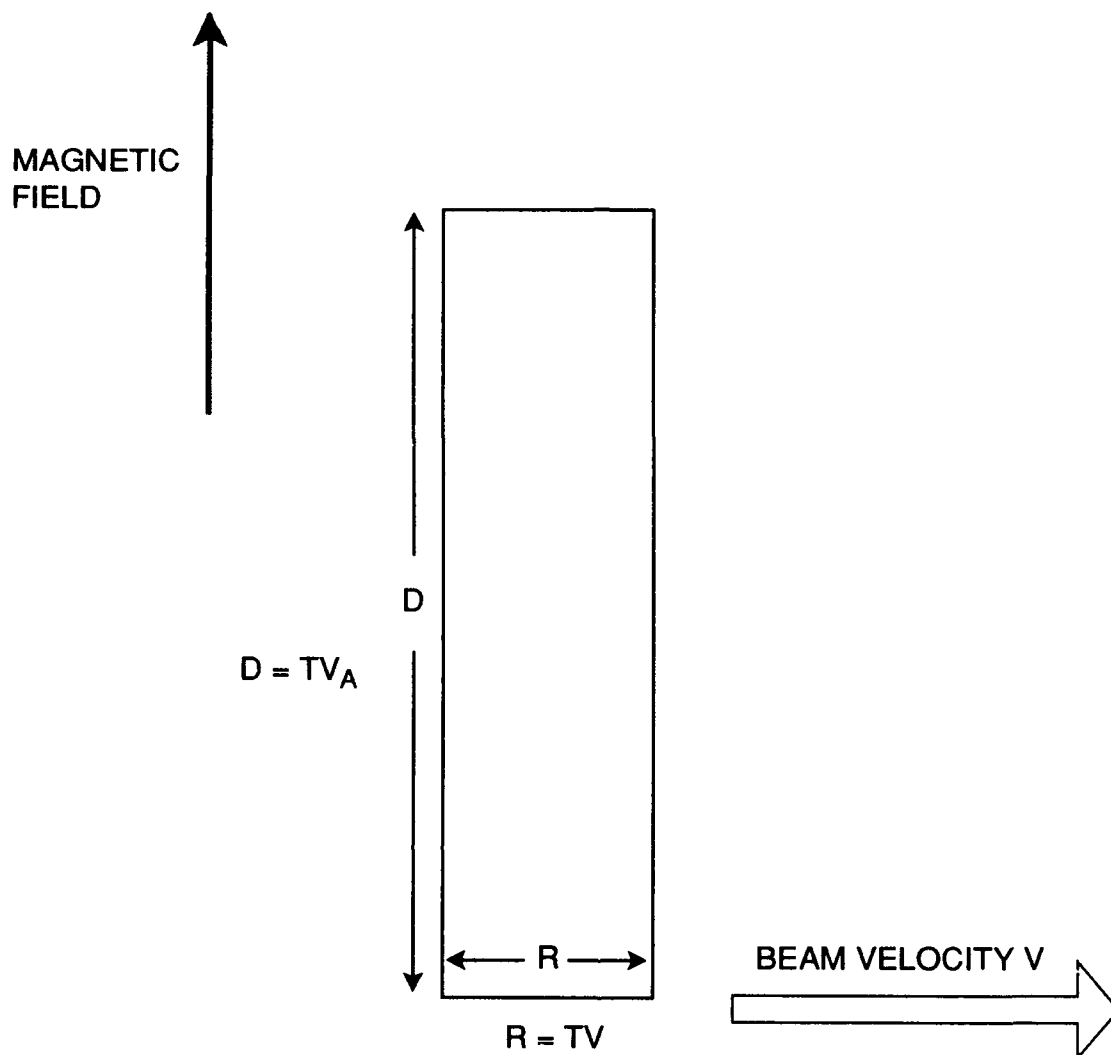


Figure 10. Momentum Coupling Between Beam Ions and the Ambient Ions in a Flux Tube

### 3.10 Computer Simulation of Xenon CIV

By using the particle-in-cell plasma simulation method<sup>25</sup> one can simulate the explicit time evolution of plasma dynamics. Earlier works on computer simulations of CIV have been reported by Machida and Goertz.<sup>26</sup> Following the approach of Machida and Goertz,<sup>25</sup> two other

<sup>25</sup> Birdsall, C.K. and Langdon, B.G. (1985) *Plasma Physics via Computer Simulation*, New York:McGraw-Hill Book Co.

<sup>26</sup> Machida, S. and Goertz, C.K. (1986) A simulation study of the critical ionization velocity process, *J. Geophys. Res.*, **91**:11965.

CIV simulation codes<sup>9,27</sup> have been written independently. These two codes, using better cross sections and taking into account full arrays of collisional mechanisms, yield the time development of CIV as a result of the interplay between collisional and plasma effects.

A limitation of the above works is the use of one-dimensional space, although their velocities are three-dimensional. Another limitation is the practice of assuming the ion to electron mass ratio to be 100. These limitations are necessary to reduce the tremendous computation time (even on modern large scale computers) required to simulate tens of thousands of interacting particles. Despite these limitations, the simulation results have been useful for providing useful physical insights into the detailed dynamics<sup>9,26,27</sup> of CIV.

The purpose of this work is to provide physical insights. We have used the explicit method as described in Machida and Goertz<sup>26</sup> and McNeil et al<sup>9</sup>. We assume that seed ions are initially present in the xenon cloud (or beam). They are formed as a result of charge exchange between Xe neutrals and ambient O<sup>+</sup>. Before we present the CIV plasma simulation results, we first present a Monte Carlo simulation of time evolution of the build up of xenon seed ions in the neutral xenon cloud as a result of charge exchange (Figure 11).

In our CIV plasma simulation, the electrons and ions are represented by "clouds of charge" moving through one another in response to the electric field created by charge separation, which is due to the "tie down" of electrons by the magnetic field lines. The electrons are pulled to some extent along with the neutrals through the polarization drift, but due to their short gyroradius are accelerated mainly along magnetic field lines. In a time scale of less than a quarter of an ion gyroperiod, the ions traverse "straight across" the field lines as if unmagnetized. In this fast time scale, the ions accomplish the transfer of much of their kinetic energy to the plasma instability waves which in turn "heat" the electrons rapidly.

The simulation is one-dimensional in displacement, allowing an electric field in only one direction. The magnetic field is applied in a direction almost perpendicular to the electric field, with a small angle  $\Theta = \sqrt{m/M}$ , where  $m$  and  $M$  are the electron and ion masses respectively. This angle is chosen for maximum growth rate of the modified two-stream instability. We have taken into account the excitation and ionization of metastable states, charge exchange, line excitation, and, of course, electron impact ionization. The simulation parameters are shown in Table 3.

<sup>27</sup> Person, J.C., Resendes, D., Petschek, H., and Hastings, D.E. (1990) Effects of collisional processes on the critical velocity hypothesis. *J. Geophys. Res.*, **95**: 4039.

P91-1 Xenon Release --- Xenon Ion Density (unmagnetized)

Vent time = 1 s. Flow Rate = 304. g/s  $\theta_{\max} = 30^\circ$

$[H^+] = 2.0E+04/cc$   $\sigma = 1.5E-16$  cm<sup>2</sup>  $V = 7.4$  km/s  $\Delta t = 0.35$  s.

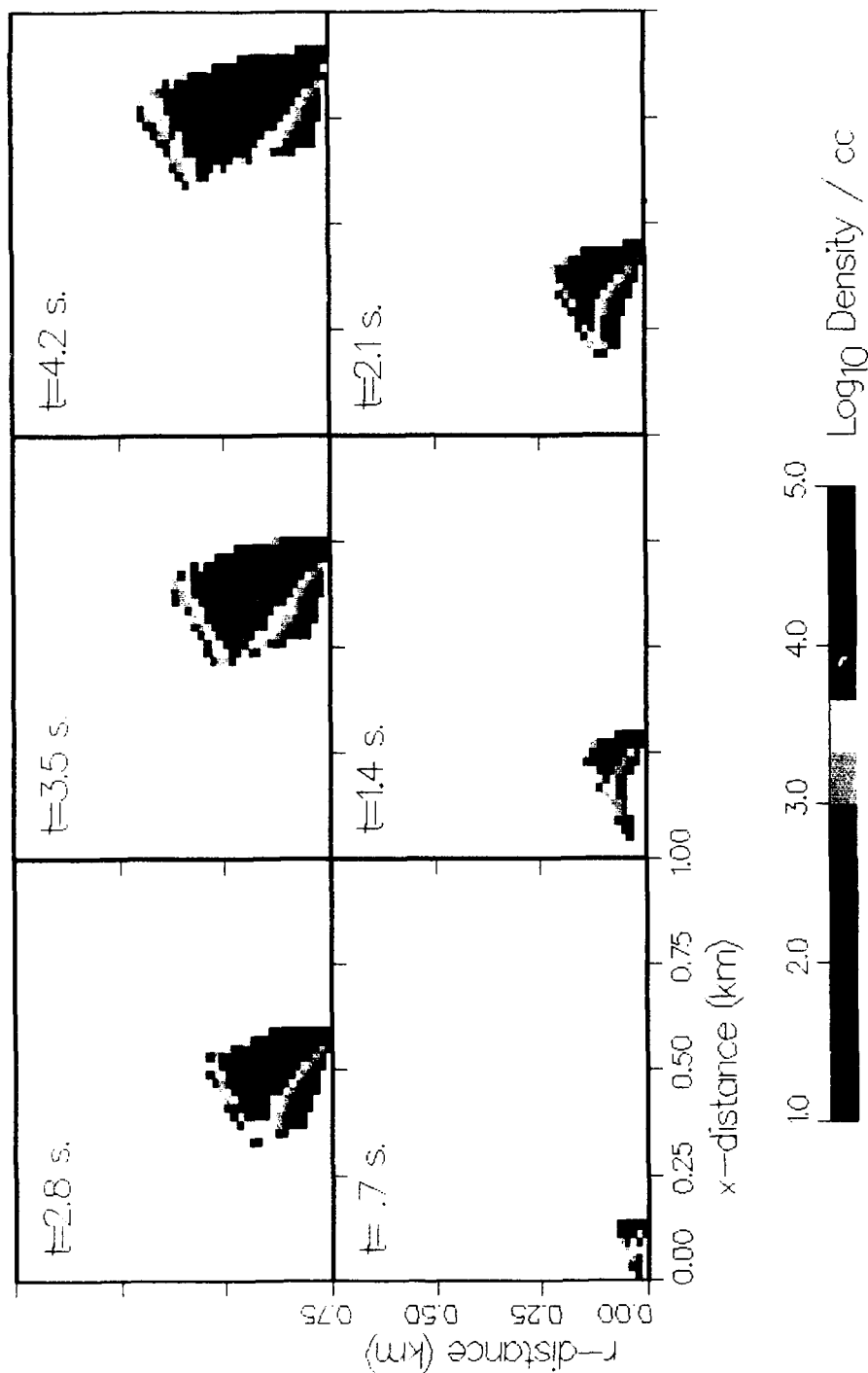


Figure 11. Simulation Results of Charge Build up in a Neutral Cloud as a Result of Charge Exchange with the Ambient Atomic  $O^+$

Table 3. Simulation Parameters

Initial Number of Particles	1024
Number of Cells	128
Ion Mass/Electron Mass	100
Initial Mass Frequency/Electron Gyrofrequency	1
Tilt Angle of Magnetic Field	6°
Beam Velocity/Critical Velocity	1.5
Reference Collision Rate/ $\omega_e$	0.2
kV/ $\omega_e$ (Primary Mode)	0.04
Ambient Ion Velocity	0.0

Typical results are shown in Figure 12. Electron (upper panel) and ion (lower panel) energies, normalized by the beam energy, are plotted as functions of time normalized by the initial plasma frequency. The neutral beam travels in time from left to right. The electrons are gaining energy from the plasma waves. As the electron energy reaches the ionization energy  $e\phi$ , ionization of the neutrals begin to occur. The new electrons are of low energy when created and they are energized to higher energies later.

### 3.11 Physical Interpretation

We observe several interesting points in the simulation results shown in Figure 12. (1) The energy and population of the electrons increase with time. This is a manifested symptom attributed to CIV. (2) The ion energy spreads. (3) There is a new observation heretofore not reported in CIV simulations studies. We observe that the growth of ionization takes off when the combined seed ionization and electron impact generated ionization densities equal the ambient plasma density approximately. (4) Taking a typical nighttime plasma frequency of  $10^6$  Hz at 800 km, the simulation shows that it would take about 2 ms for CIV to take off. For a 200 m/s beam velocity, this means about 4 m from the nozzle.

The behavior (3) may be explained by means of the standard linear theory of beam-plasma instability.<sup>28</sup> In the low beam density regime ( $\omega_b \ll \omega_a$ ), where  $\omega_b$  and  $\omega_a$  are beam and ambient plasma frequencies respectively, the modified two-stream instability dispersion relation yields the solution:

$$\omega_r = kV - \frac{\omega_i}{\sqrt{3}} \quad (15)$$

<sup>28</sup> Mikhailovskii, A.B. (1974) *Theory of Plasma Instabilities*, Vol. 1, Consultant Bureau, N.Y.

1991-11-29 14:42:45

NE=1024 NX=128 L= 6.28 WP= 1.0 WC= 1.0  
 A= 6.00 VO= 0.04 IMLCE1110 Rs=0.002 I/E= 100.  
 B/I= 1.5 NU0 =0.200 Ma= 0.25 Va= 0.00

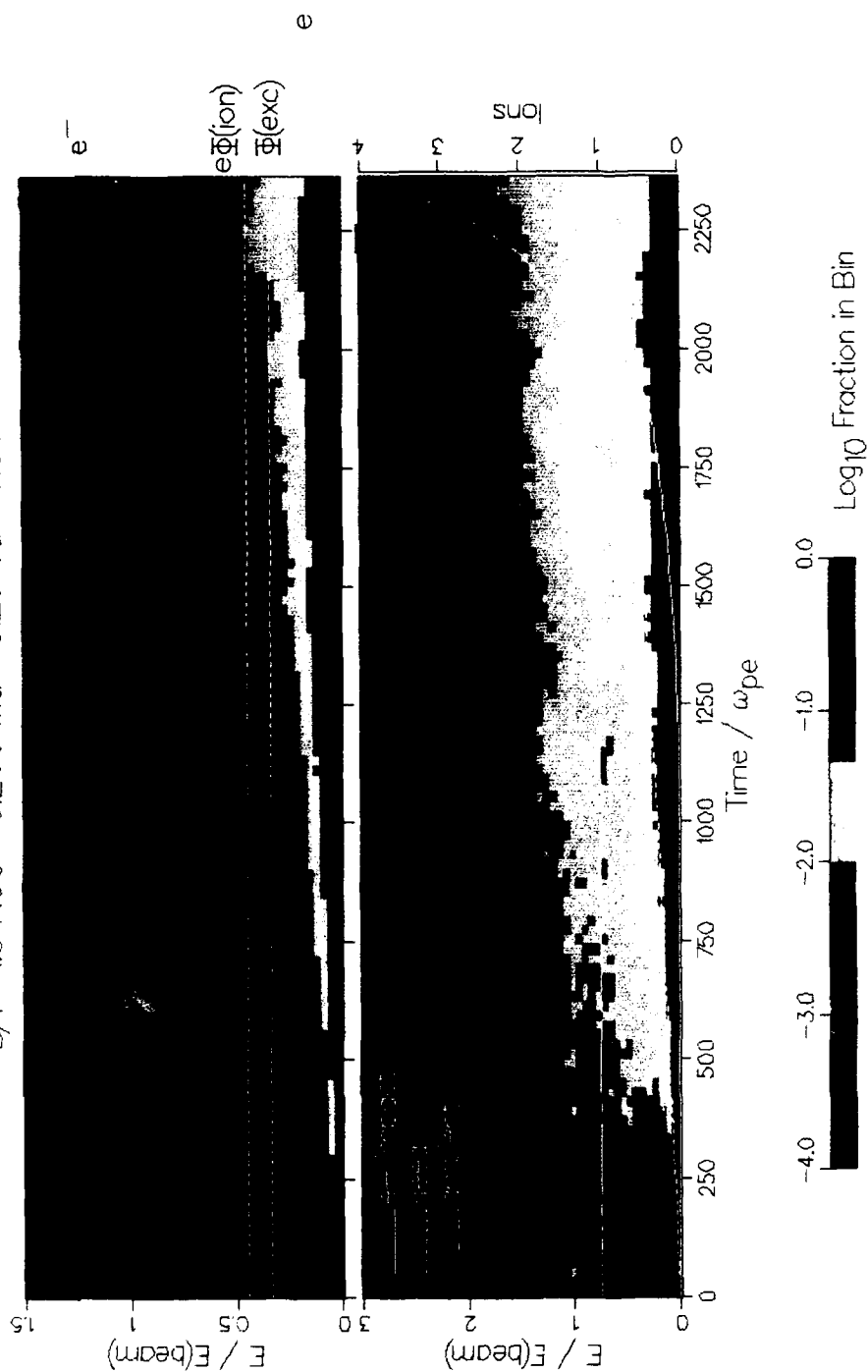


Figure 12. Simulation Results of Xenon CIV. Metastable states, line excitation, charge exchange, and of course, electron impact ionization have been taken into account

where

$$\omega_i = \frac{\sqrt{3}}{2} \omega_{LH} (1 + \delta^2)^{1/6} \left(\frac{\epsilon}{2}\right)^{1/3}. \quad (16)$$

where  $\omega_{LH}$  is the lower hybrid frequency;  $r$  and  $i$  denote the real and imaginary parts respectively.

$$\delta = \sin\theta \sqrt{\frac{M}{m}}. \quad (17)$$

and

$$\epsilon = \frac{\omega_b^2}{\omega_a^2}. \quad (18)$$

In the higher beam density regime ( $\omega_b \geq \omega_a$ ), the solution is given by

$$\omega_r = \frac{\sqrt{3}}{2} \omega_{LH} \quad (19)$$

$$\omega_i = \frac{1}{2} \omega_{LH}. \quad (20)$$

Physically, the ionization rate does not take off until the total beam plasma density (seed + electron impact ionizations) approximately equals the ambient plasma density.

As a corollary to the above theorem, if one can artificially seed a neutral beam by artificial means (such as by using samarium,<sup>29</sup> for example) to speed up the increase of beam ion density, it would trigger CIV more quickly. We believe that this point is worth pursuing for further research.

---

<sup>29</sup> Lal, S.T., Murad, E., and McNeil, W.J. (1992) Amplification of critical velocity ionization by associative ionization, *J. Geophys. Res.*, **97**: (No. A4) 4099-4108.



#### 4. CARBON DIOXIDE GAS RELEASE

The purpose of the CO<sub>2</sub> gas release in the proposed experiment on ARGOS is not CIV but to observe signatures of collisional excitation of CO<sub>2</sub> with atmospheric O and H atoms. The reason that CO<sub>2</sub> will not undergo CIV in this experiment is that the critical ionization velocity  $V_*$  (= 7.9 km/s) of CO<sub>2</sub> exceeds the CO<sub>2</sub> gas velocity in the space frame. The magnitude of the maximum vector sum of the satellite velocity  $V_s$  (7.4 km/s) and the gas velocity  $V_g$  (0.4 km/s) is only  $|V_s + V_g| = 7.8$  km/s. Even in sunlight, CO<sub>2</sub> cannot be photolionized by the Lyman- $\alpha$  line of sunlight because the ionization energy [ $\Phi(\text{CO}_2) = 13.8$  eV] of CO<sub>2</sub> exceeds the energy ( $h\nu = 10.2$  eV) of Lyman- $\alpha$ .

##### 4.1 Reaction with Atmospheric Species

The 800 km altitude of ARGOS is ideal for studying two important reactions: the reaction of O atoms and the reaction of H atoms. In the first case, vibrationally-excited CO is produced, while in the latter case vibrationally-excited OH is produced:



These reactions give rise to emissions at the fundamentals of CO(4.6 $\mu$ ) and OH(2.7 $\mu$ ) as well as the overtones.

##### 4.2 Reaction Energetics

The kinetic energy available for a collisional reaction [such as Eq. (21) or Eq. (22)] between two masses is the kinetic energy  $E_{\text{CM}}$  in the center of mass frame. By conservation of momentum,

$$E_{\text{space}} = (1 + M_B/M_O)E_{\text{CM}}. \quad (23)$$

Figure 13 shows the range,  $(E_b, E_f)$  of kinetic energy  $E_{CM}$  available for the reaction [Eq. (21)], the upper limit,  $E_f$ , corresponding to the forward release and the lower one,  $E_b$ , to the backward release. As a consequence of excitation of the spectral lines in the energy range,  $(E_b, E_f)$ , the optical signatures of the forward and backward releases are expected to be different. Similarly, Figure 14 shows the energy range for reaction [Eq. (22)]. Figure 15 shows some of the spectral lines<sup>30</sup> of the reaction [Eq. (21)] in the range,  $(E_b, E_f)$ .

### 4.3 Monte Carlo Simulation

Setayesh<sup>31</sup> has calculated the emissions of reactions [Eq. (21) and Eq. (22)] and used a numerical plume simulation code<sup>32</sup> to obtain the spatial distribution of the emission in the plume of such a release (Figures 16,17). Setayesh's results indicate that both of these processes [Eq. (21), Eq. (22)] would be observable from the ground.

Electron impact excitation of  $CO_2$  may also occur. In the  $CO_2$  gas release, even though the relative velocity between the gas and the ambient plasma is just below the critical ionization velocity,  $V_c$ , plasma instability may occur. The gas can form an ion beam in two ways: (1) charge exchange between  $CO_2$  and the ambient ions, and (2) ambient ion reflection. The ambient ions are  $O^+$  when in sunlight or  $H^+$  at night.

Such an ion beam, which is generated by non-CIV processes, can generate some CIV-like signatures even when the beam velocity is below the CIV requirement. It can also amplify a CIV process if the latter is taking place.<sup>29</sup> The ion beam, traversing the ambient magnetized plasma, can excite plasma instability, thereby energizing the electrons. Some of the energetic electrons may be able to excite or even ionize the gas, even though a sustained cyclic ionization process is not expected because of the subcritical velocity  $V(CO_2)$  used in the experiment.

<sup>30</sup> Orient, O.J., Chujian, A., and Murad, E. (1990) Reaction and electronic excitation in crossed-beams collisions of low energy  $O(^3P)$  atoms with  $H_2O$  and  $CO_2$ , *Phys. Rev. Lett.*, **65**:No 19, 2359-2361.

<sup>31</sup> Setayesh, A. (1991) A parametric study of the release of  $CO_2$  in space, Report PL-TR-91-2052, Phillips Laboratory, Hanscom AFB, MA ADA-236271.

<sup>32</sup> Elgin, J.B., Cooke, D.C., Tautz, M.F., and Murad, E. (1990) Modeling of atmospherically induced gas phase optical contamination from orbiting spacecraft, *J. Geophys. Res.*, **95**:12197-12208.

## 5. CONCLUSION

In our proposed experiment, xenon and carbon dioxide gases will be released from the ARGOS satellite. The xenon gas release will be used to test Alfvén's hypothesis of CIV. If CIV occurs, we expect the energetic electrons to excite the  $\text{Xe}^+$ , with subsequent radiation. The carbon dioxide gas release will be used to test reactions with atmospheric O and H atoms. The radiation will be observed at Maui and possibly on the satellite.

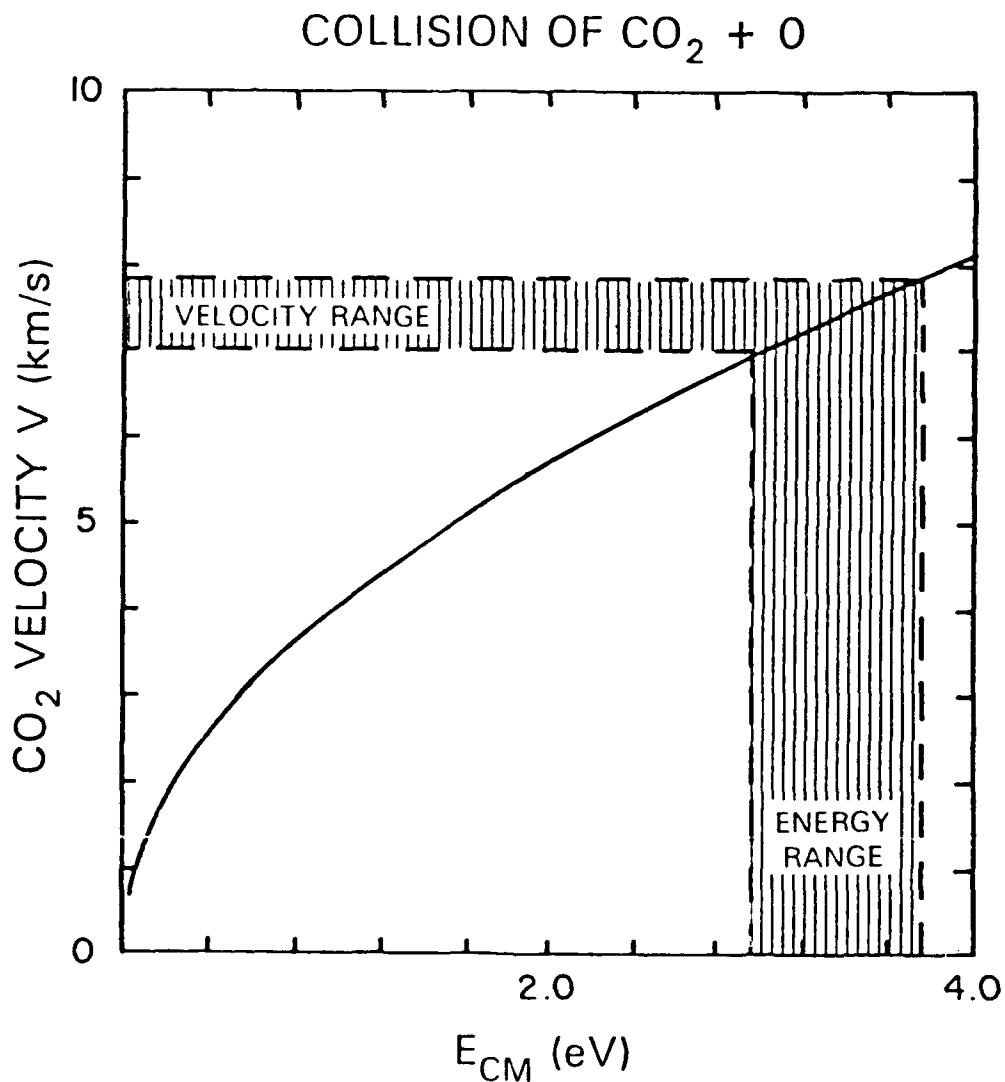


Figure 13. The Center of Mass Energy Range, Bracketed by the Forward and Backward Release Cases, for the Collision  $\text{CO}_2 + \text{O}$

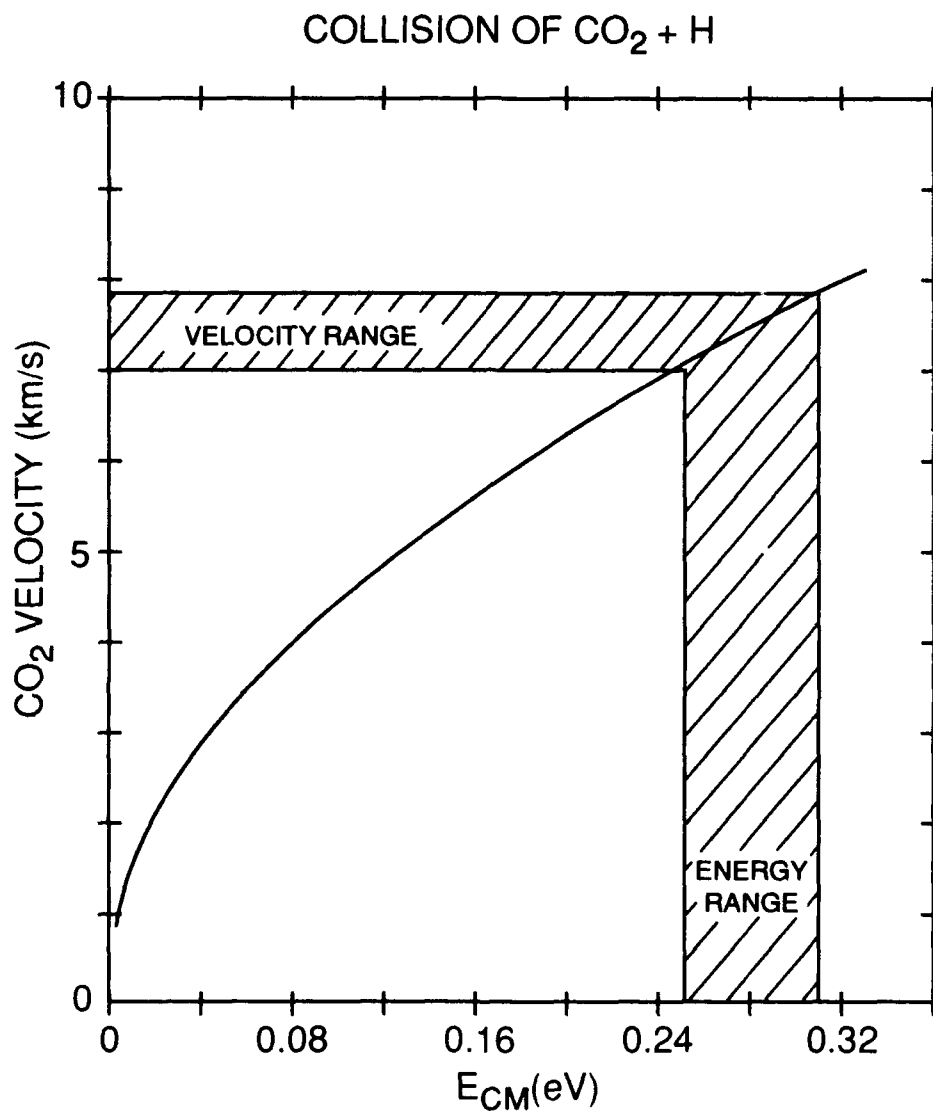


Figure 14. The Center of Mass Energy Range, Bracketed by the Forward and Backward Release Cases, for the Collision  $\text{CO}_2 + \text{H}$

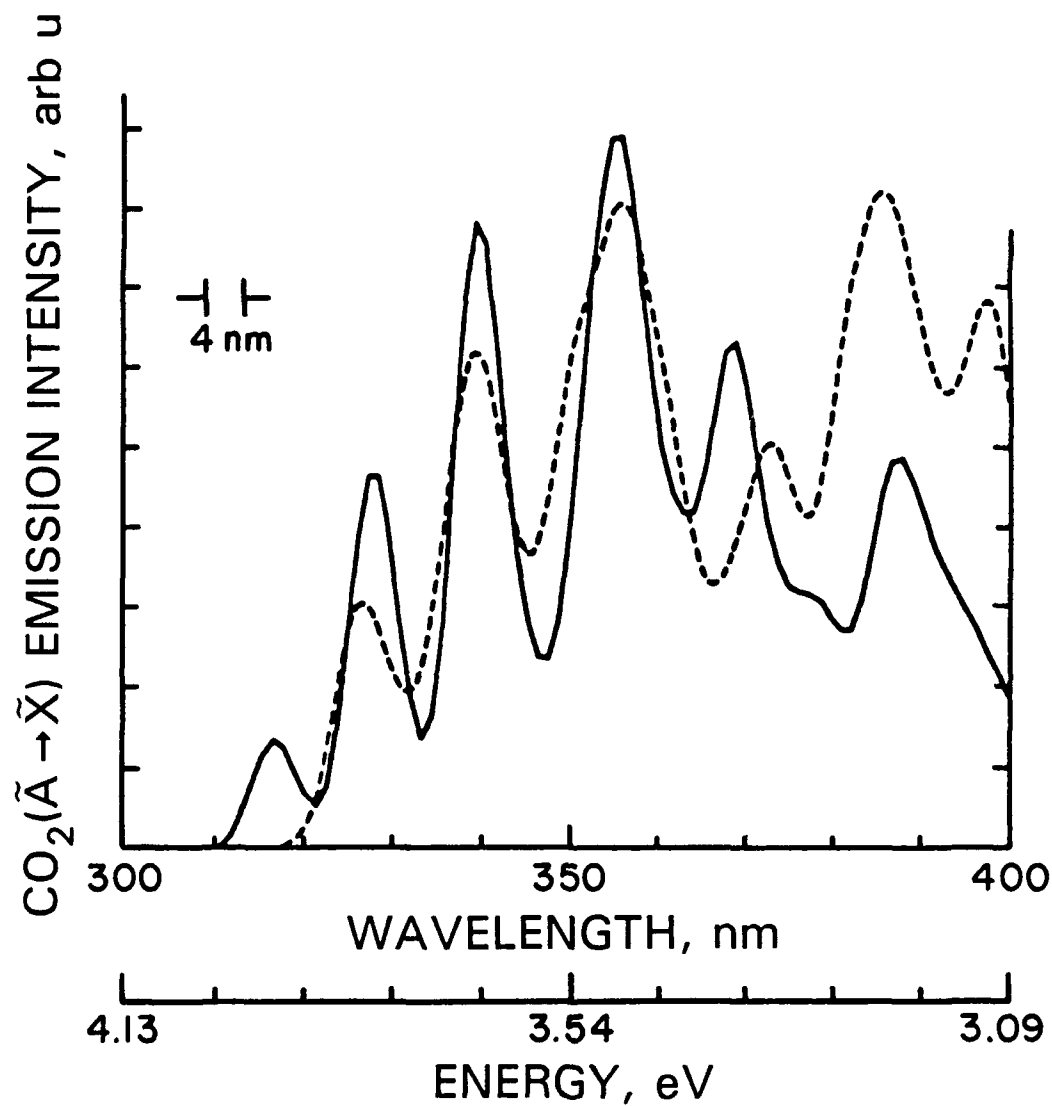


Figure 15. Experiment (-) and Calculated (---) Emission Spectra in the  ${}^1B_2 \rightarrow {}^1A_1$  Transition of  $\text{CO}_2$  for the Collision  $\text{CO}_2 + \text{O}$  [from Orient et al, 1990]

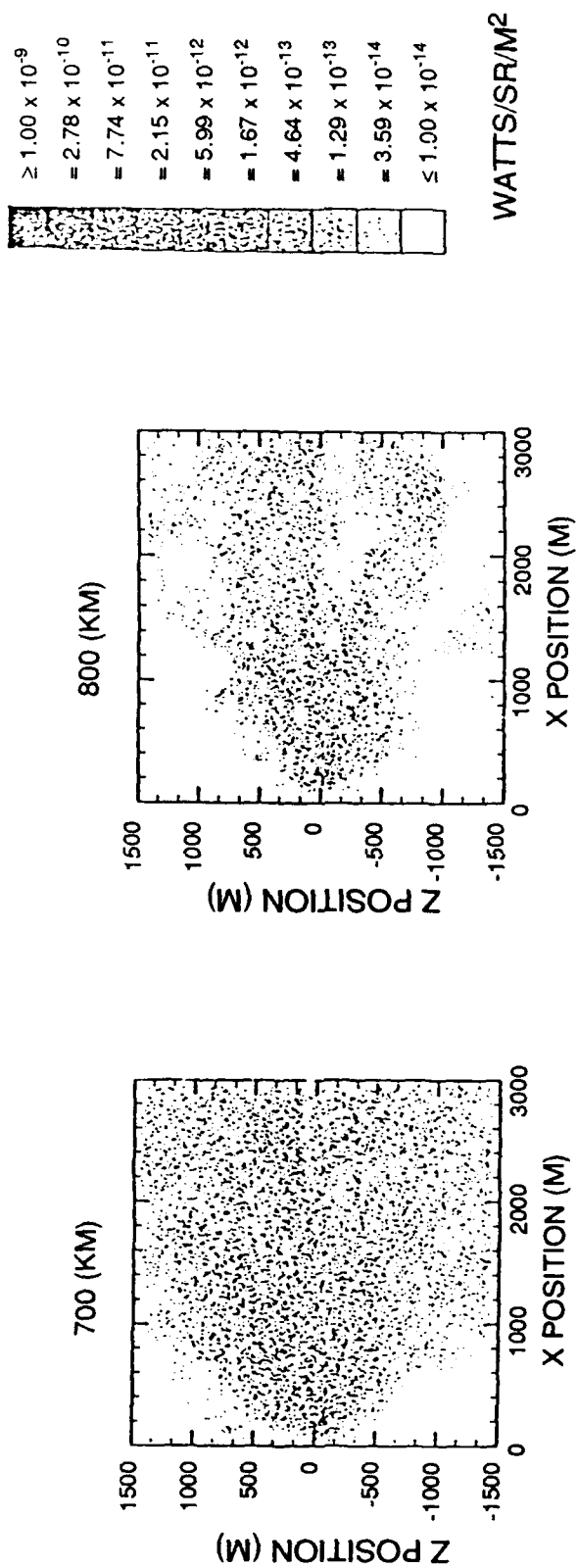


Figure 16. Results of Monte Carlo Simulation of  $\text{CO}_2 + \text{O} \rightarrow \text{CO}^* + \text{O}_2$  Showing the CO Vibrational Emission at  $4.6 \mu\text{m}$

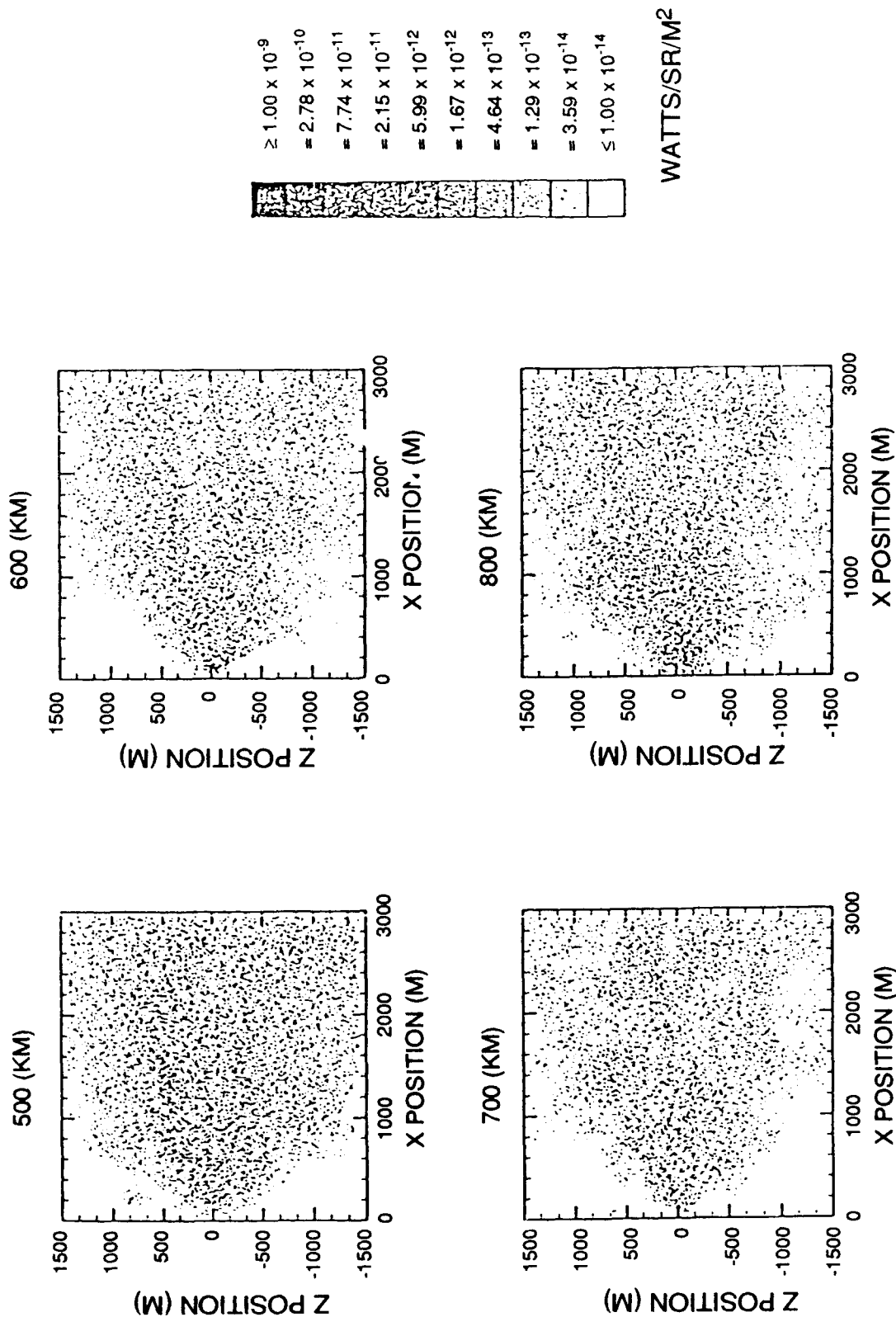


Figure 17. Results of Monte Carlo Simulation of  $\text{CO}_2 + \text{H} \rightarrow \text{OH}^* + \text{CO}$  Showing the OH Vibrational Emission at 2.7  $\mu\text{m}$

## References

1. Bernhardt, P., Tepley, C.A., and Duncan, L.M. (1989) Airglow enhancements associated with plasma cavities formed during ionospheric heating experiments, *J. Geophys. Res.*, **94**:9071.
2. Alfvén, H. (1960) Collision between a non-ionized gas and a magnetized plasma, *Rev. Mod. Phys.*, **32**:710-713.
3. Alfvén, H. (1954) *On the Origin of the Solar System*, Oxford Univ. Press, Oxford.
4. Möbius, E., Boswell, R.W., Piel, A., and Henry, P. (1979) A spacelab experiment on the critical ionization velocity, *Geophys. Res. Lett.*, **6**:29.
5. Axnäs, I. (1980) Some necessary conditions for a critical velocity interaction between the ionospheric plasma and a xenon cloud, *Geophys. Res. Lett.*, **7**:933-936.
6. Murad, E., Lai, S.T., and Stair, A.T. (1986) An experiment to study the critical ionization velocity theory in space, *J. Geophys. Res.*, **91**:A9 10188-10192.
7. Möbius, E., Papadopoulos, K., and Piel, A. (1987) On the turbulent heating and the threshold condition in the critical ionization velocity interaction, *Planet. Space Science*, **35**:345.
8. Goertz, C.K., Machida, S., and Lu, G. (1990) On the theory of CIV, *Adv. Space Res.*, 33-46.
9. McNeil, W.J., Lai, S.T., and Murad, E. (1990) Interplay between collective and collisional processes in critical velocity ionization, *J. Geophys. Res.*, **95**:A7 103435-10354.
10. Formisano, V., Galeev, A.A., and Sagdeev, R.Z. (1982) The role of the critical ionization velocity phenomenon in the production of the inner coma cometary plasma, *Planet. Space Sci.*, **30**:491-497.
11. Jönsson, B.O. (1980) private communication to I. Axnäs.
12. de Heer, F.J., Jansen, R.H.J., and van der Kaay, W. (1979) *J. Phys. B*, **12**:979-1002.
13. Reidl, P.C. (1988) *Thermal Physics*. 2nd edition, Oxford University Press, Oxford.



14. Townsend, J.S. (1915) *Electricity in Gases*, Clarendon Press, Oxford.
15. Lai, S.T. and Murad, E. (1992) Inequality conditions for critical velocity ionization space experiments, *IEEE Trans. Plasma Sci.*, in press.
16. Lai, S.T. and Murad, E. (1989) Critical ionization velocity experiments in space, *Planet. Space Sci.*, **37**:7/865-872.
17. Brenning, N. (1982) Comment on the Townsend condition, presented at the Workshop on Alfvén's Critical Velocity Effect, Max-Planck Institut für Extraterrestrische Physik, Garching, W. Germany.
18. Tanaka M. and Papadopoulos, K. (1983) Creation of high energy tails by means of the modified two-stream instability, *Phys. Fluids*, **26**:1697.
19. Tobert, R.B. (1990) Review of critical velocity experiments in the ionosphere, *Adv. Space Res.*, **10**:7/47-58.
20. Newell, P.T. and Torbert, R.B. (1985) Competing atomic processes in Ba and Sr injection critical velocity experiments, *Geophys. Res. Lett.*, **12**:835.
21. Lai, S.T., Murad, E., and McNeil, W.J. (1991) Altitude effects in CIV experiments in space, *Planet. Space Sci.*, **39**:12 1707-1713.
22. Haerendel, G. (1982) Alfvén's critical velocity effect tested in space, *Z. Naturforsch.*, **37A**:728.
23. Haerendel, G. (1983) The role of momentum transfer to the ambient plasma in critical velocity experiments, Active Experiments in Space, *Eur. Space Agency Spec. Publ.*, **ESA SP-195**:245.
24. Kashe, M.A. (1969) *The Ionosphere and Its Interaction with Satellites*, Gordon and Breach, NY.
25. Birdsall, C.K. and Langdon, B.G. (1985) *Plasma Physics via Computer Simulation*, New York:McGraw-Hill Book Co.
26. Machida, S. and Goertz, C.K. (1986) A simulation study of the critical ionization velocity process, *J. Geophys. Res.*, **91**:11965.
27. Person, J.C., Resendes, D., Petschek, H., and Hastings, D.E. (1990) Effects of collisional processes on the critical velocity hypothesis, *J. Geophys. Res.*, **95**: 4039.
28. Mikhailovskii, A.B. (1974) *Theory of Plasma Instabilities*, Vol. 1, Consultant Bureau, N.Y.
29. Lai, S.T., Murad, E., and McNeil, W.J. (1992) Amplification of critical velocity ionization by associative ionization, *J. Geophys. Res.*, **97**: (No. A4) 4099-4108.
30. Orient, O.J., Chujian, A., and Murad, E. (1990) Reaction and electronic excitation in crossed-beams collisions of low energy O(<sup>3</sup>P) atoms with H<sub>2</sub>O and CO<sub>2</sub>, *Phys. Rev. Lett.*, **65**:No 19, 2359-2361.
31. Setayesh, A. (1991) A parametric study of the release of CO<sub>2</sub> in space, Report PL-TR-91-2052, Phillips Laboratory, Hanscom AFB, MA ADA-236271.
32. Elgin, J.B., Cooke, D.C., Tautz, M.F., and Murad, E. (1990) Modeling of atmospherically induced gas phase optical contamination from orbiting spacecraft, *J. Geophys. Res.*, **95**:12197-12208.